9

Polymer-Based EMI Shielding Materials

Chong Min Koo[1,2,3], Faisal Shahzad[1,2,4], Pradip Kumar[1], Seunggun Yu[1], Seung Hwan Lee[1], and Jun Pyo Hong[1]*

[1] *Center for Materials Architecturing, Korea Institute of Science and Technology, Seoul, Republic of Korea*
[2] *Nanomaterials Science and Engineering, University of Science and Technology, Daejeon, Republic of Korea*
[3] *KU-KIST Graduate School of Converging Science and Technology, Korea University, Seoul, Republic of Korea*
[4] *National Center for Nanotechnology, Department of Metallurgy and Materials Engineering, Pakistan Institute of Engineering and Applied Sciences (PIEAS), Islamabad, Pakistan*

Abbreviations

ABS	Acrylonitrile–butadiene–styrene
CB	Carbon black
CF	Carbon fiber
CNFs	Carbon nanofibers
CNTs	Carbon nanotubes
EG	Expanded graphite
EMI	Electromagnetic interference
f	Frequency
Fe_3O_4	Magnetite, Iron oxide
FeO	Iron oxide
GO	Graphene oxide
ICPs	Intrinsically conducting polymers
MG	Magnetic graphene
MLG	Multilayer graphene sheets
PA	Polyamide
PANI	Polyaniline
PC	Polycarbonate
PCL	Polycaprolactone
PDMS	Poly(dimethylsiloxane)
PE	Polyethylene
PEDOT	Poly(3,4-ethylenedioxythiophene)
PEI	Polyethyleneimine
PEO	Poly(ethylene oxide)
PES	Poly(ether sulfone)

* Corresponding author: E-mail address: koo@kist.re.kr (C.M. Koo).

Advanced Materials for Electromagnetic Shielding: Fundamentals, Properties, and Applications, First Edition.
Edited by Maciej Jaroszewski, Sabu Thomas, and Ajay V. Rane.

PET	Poly(ethylene terephthalate)
PI	Polyimide
PMMA	Poly(methyl methacrylate)
PP	Polypropylene
PPy	Polypyrrole
PS	Polystyrene
PTP	Polythiophene
PTT	Poly(trimethylene terephthalate)
PU	Polyurethane
PVA	Poly(vinyl alcohol)
PVC	Poly(vinyl chloride)
PVDF	Poly(vinylidene fluoride)
rGO	Reduced graphene oxide
RL	Reflection loss
SAN	Styrene acrylonitrile copolymer
SBS	Styrene–butadiene–styrene
SE	Shielding effectiveness
SEBS	Styrene–ethylene/butylene–styrene
SWCNT	Single-walled carbon nanotube
t	Thickness
UHMWPE	Ultra-high molecular weight polyethylene
σ	Conductivity

9.1 Introduction

9.1.1 Need for Polymer-Based EMI Shielding Materials

Modern electronic devices have sparked the electromagnetic (EM) waves that are in our surroundings to such an extent that it has now become a severe challenge to mitigate their harmful effects in protecting the devices and to counter their negative health effects [1–3]. Several types of shielding products are currently in use and under investigation for their potential characteristics to challenge these problems. Metals, due to their extremely large electrical conductivity, have been a natural choice for electromagnetic interference (EMI) protection. However, their large cost, difficulty in processing, high density, corrosivity, and some other related problems have attracted researchers' attention to materials beyond metals in search of new options [4, 5]. Ferrites and other inorganic materials, which provide a large microwave absorption through contribution to the electric and magnetic losses, are also investigated in the quest to solve EMI problems [6, 7].

One of the leading candidates for materials as EMI shielding are polymer composites because of their numerous advantages over their counterparts in terms of cost, density, and ease of processing [2]. One often ignored advantage of polymer composites over metals is the ability to shield EM waves through absorption as the dominant phenomenon rather than reflection. This characteristic is important when a device producing EM signals need to protect itself as well as to restrict the reflecting radiation from interfering with the operation of other nearby devices. Such a characteristic is mainly suitable in military sector applications such as for camouflage or in stealth technology.

Polymers can generally be classified into two types of insulating and intrinsically conducting polymers (ICPs). Most polymers, including polystyrene (PS), poly(vinylidene fluoride) (PVDF), polypropylene (PP), poly(methyl methacrylate) (PMMA), poly(vinyl alcohol) (PVA), polyethylene

(PE), poly(vinylpyrrolidone) (PVP), and epoxy are generally insulating polymers and therefore need to be compounded with conducting fillers to increase their conductivity to meet the requirements for EMI shielding. Metallic nanowires (silver, nickel, copper, and steel) were initially used as filler to impart the metallic conduction character to insulating polymers. However, the difficulty of processing, poor dispersion, and insignificant interaction of filler material with host matrix, which leads to poor mechanical properties, suggest the use of carbonaceous fillers as replacements [5, 8]. Several conductive coatings and metal platings over plastics were also used to provide the required EMI shielding; however, additional steps to fabricate the plastic surface and fabrication procedures led to the use of other conductive additives, which will be discussed below.

Intrinsically conducting polymers are conjugated polymers that exhibit electronic properties when they are doped. They are another suitable candidate for EMI shielding [3] that is attracting further attention from research communities as a polymer matrix to be converted from an insulating into a conducting materials. Whilst the synthesis, cost, and availability of ICPs has yet to reach the optimum level of commercialization, the ongoing research trends still greatly use these polymers. Among the conducting polymers, polyaniline (PANI), polypyrrole (PPy), and poly(3,4-ethylenedioxythiophene) (PEDOT) are the most explored for EMI shielding applications. Similar to insulating polymers, nevertheless, the ICPs are also explored as polymer composite material with several conducting fillers due to their insufficient EMI SE. Among the filler materials, most researches have focused on carbon derivatives. Graphite, carbon black (CB), carbon nanotubes (CNTs), carbon nanofibers (CNFs), and more recently graphene, have mostly been investigated for EMI shielding applications [2]. Inorganic fillers, such as ferrites (Ni, Zn, Mn), magnetic iron nanoparticles (Fe_2O_3, Fe_3O_4), and other metal oxides (SnO_2, TiO_2, ZnO) were also explored to enhance the microwave absorption ability of polymer composites through increasing the magnetic loss contribution [9–11]. Several efforts to use polymer blends in conjunction with conductive fillers were also reported in order to obtain maximum output in terms of shielding efficiency [12, 13].

The structural design of polymer composite is most important as several constituents influence the contribution of individual properties of filler materials. The unique properties that can emerge from filler–filler or filler–polymer interactions provide new opportunities to design hybrid polymer materials. A key requirement for EM waves to be absorbed in the material is achieved when the impedance of air matches that of the shielding material. This is generally not straightforward as there is always a difference in polarizing ability between air and the material under test; however, this can be achieved to a certain extent by introducing a cellular foam structure in the polymer matrix [14]. Foams, in addition to providing air in the gaps of matrix, also decrease the density, which in turn increases the specific EMI SE values of polymer composites.

Another approach to manufacturing EMI shielding materials is to use the entire conductive material with full continuity, such as conductive Bucky papers [15, 16]. A lamellar structure has been proposed by several authors in which a conductive sheet is placed between two insulating polymeric sheets [17]. The performance of an insulating polymer relies heavily on the conductive filler type and its content [2]. Formation of a continuous conducting network structure is generally what is required to provide optimum properties. When the filler content is gradually increased in an insulating matrix, the conductivity of the resulting composite gradually increases and reaches a critical value, often called the percolation limit or insulator/conductor transition limit. The percolation limit, depending on the filler content, also takes into account the nature of the filler material, such as the aspect ratio, its intrinsic conductivity, and interaction with host matrix. Further increase in filler content beyond the percolation limit will dramatically increase the electrical conductivity. The key point is the formation of conducting pathways and filler-to-filler contacts inside the insulating matrix. This kind of percolation

behavior is, however, not present in ICPs. Several approaches have recently been used to obtain such filler-to-filler contact using segregated structures and aligned fillers [18, 19]. Deployment of a continuous network of thermally or electrically conductive fillers using a core–shell polymer structure is one such approach that has been used to enhance the properties.

9.1.2 Factors Effecting EMI SE

The ideal material for EM wave absorption should have certain characteristic to mitigate the EMI shielding problems. First, impedance matching between free space (air) and the surface of a shielding material can help with propagation of the wave into the material, thus hindering the reflection. Second, the shielding material should possess substantial dielectric and magnetic loss properties to absorb the electromagnetic waves [2, 14, 20].

Electromagnetic radiation at high frequencies penetrates only in the near surface region of an electrical conductor. This is known as the skin effect. The electric field intensity of a plane wave penetrating into a conductor decreases with depth of the conductor. The depth at which the field decreases to 1/e times of the incident value is called the skin depth (δ), given by Equation 9.1:

$$\delta = \left(\sqrt{\pi f \sigma \mu}\right)^{-1} \tag{9.1}$$

where f = frequency, μ = magnetic permeability ($\mu = \mu_0\mu_r$), μ_r = relative magnetic permeability, $\mu_0 = 4\pi \times 10^{-7}$, and σ = electrical conductivity in $S{\cdot}m^{-1}$. For this reason, the skin depth decreases with increasing frequency and with increasing conductivity or permeability [4].

Polymer composites with large dielectric constants are ideal candidates to provide a dielectric loss contribution because of the conductivity mismatch between conductive filler and insulating polymeric matrix. According to the Maxwell–Wagner–Sillars (MWS) principle, the difference between the electrical conductivities of two adjacent materials results in polarization and charge accumulation at their interfaces. Therefore, as a synergistic benefit, it is possible to get a high k value material with highly conductive fillers in an insulating matrix. The type of filler and orientation of particles in a particular direction can also increase the polarization ability of a polymer system [21].

Another important factor, similar to dielectric polarizability, is the permeability. Materials with large permeability or magnetic loss tend to absorb more EM waves. Generally, complex permittivity and permeability are the two connected features required for EMI shielding materials. Electrical conductivity, on the other hand, is the foremost parameter for any material used for EMI shielding. While EMI absorption is possible using EM wave absorbers, such as ferrites, sufficient EMI SE cannot be achieved without the material being electrically conductive. All efforts to design a suitable material for EMI shielding require high electrical conductivity as a prime parameter. A simple rule of thumb is that larger electrical conductivity leads to higher EMI SE. However, there is no direct relationship of electrical conductivity with SE as several other factors, such as thickness and dielectric properties, play important roles in determining the net EMI SE.

Similarly, in designing the polymer composites, it is important to take into consideration the nano-effects originating from components with nanosize dimensions. Nanoparticles are known to provide better electrical, magnetic, and optical properties. When the particle size of the filler is below the skin depth, the eddy current loss can be induced, which in turn can raise the microwave absorption property of the composite system [20]. Frequency also influences the EMI SE values. Theoretically, the shielding due to absorption increases with the increase of frequency; therefore, some polymer composite systems are more suitable to shield the devices against EM waves at high frequencies [22].

Among the non-intrinsic parameters, thickness is another controlling factor for EMI SE. High values of EMI SE can be obtained simply with increasing the thickness of the material; however, there is always some limitation in this regard when taking the cost and density requirements into account. This parameter is particularly important in aerospace applications where weight is an important matter.

9.2 Types of Polymer Matrixes

9.2.1 Insulating Polymers

Polymers in general can be classified into two groups: insulating and ICPs. Most polymers are electrically insulating, including but not limited to PS, PVDF, PP, PMMA, PVA, PE, PVP, and epoxy. The insulating polymers are classified into thermoplastic and thermoset, depending on their intrinsic thermomechanical properties and their behaviors on heating. Thermoplastic polymers are thermally plastic, which means that they soften when heating. Most common polymers are thermoplastic, such as PE, PP, and PS, which are considered as the simplest macromolecular chain models. These polymers are extremely attractive to various engineering fields due to their excellent processability and mechanical properties. Furthermore, high performance thermoplastics, also known as engineering plastics, have been developed to provide the advanced properties of thermal and chemical stability and excellent mechanical strength for a particular application. Polyamide (PA), polyacetal, poly(phenylene sulfide) (PPS), and poly(ethylene terephthalate) (PET) are typical engineering plastics.

Thermosetting resins are polymer compounds with crosslinked macromolecular chains, leading to a 3D network structure. The complex molecular structure enhances thermal stability and chemical resistance when the crosslink density increases owing to their structural irreversibility and durability. Thermosetting polymers, such as polyester, epoxy, and melamine formaldehyde resins, are widely used as packaging materials, which require impact strength, dimensional stability, and shape stability.

However, an insulating polymer cannot be used by itself for EMI shielding applications. As shown in Table 9.1, the insulating polymers have relatively very small EMI SE values, which are attributed to their poor electrical conductivity.

9.2.2 Intrinsically Conducting Polymers

Shirakawa, MacDiarmid, and Heeger observed that polyacetylene upon doping with iodine provides an extremely large electrical conductivity of $1.7 \times 10^5\,S\,cm^{-1}$, which is comparable to that of several metals [29]. After that, many research efforts were focused on finding new classes of conducting polymers with ecofriendly synthesis methods and great mechanical, optical, and electrical properties. Especially, their electrical capability has opened up new prospects in the fields of cutting-edge device technologies, such as sensors, actuators, solar cells, and memory devices, as well as engineering materials, such as conductive adhesive, electromaterials, and EMI shielding materials to replace metals.

As-synthesized conducting polymers exhibit relatively low electrical conductivity with a high band gap. Through a doping process, which generates charge carrier, a conducting polymer becomes highly conductive. In the doped polymer, the π-electron easily passes from valence band to conduction band as a result of a reduced energy barrier. This excited electron causes delocalization in the molecule, leading to conduction by mobile electrons. The dissociated π interaction with free radicals is observed along the one-directional polymer chain; therefore, this conduction is defined as hopping conduction by quasi one-dimensional transport [26].

Conducting polymers with various structures have been developed recently. Among the aromatic-compound-based conducting polymers, especially PANI [26], polythiophene (PTP) [28], and PPy [27] have several advantages of notably high electrical conductivity, good processability, and thermal/chemical stability.

Among these important conducting polymers, PANI has attracted attention because of its simple and ecofriendly synthesis, environmental stability, and facile doping process to reach adequate electrical conductivity. At the oxidation state during synthesis, PANI with a band gap of 3.9 eV is divided into pernigraniline, emeraldine, and leucoemeraldine bases. Especially, the emeraldine base possesses a half-oxidation state, which facilitates control of the doping level with various dopants. Based on these advantages, PANI is preferentially used in the field of EMI shielding applications.

Hong et al. reported the synthesis of EMI materials from emeraldine-base PANI film doped with hydrochloric acid prepared from solution in *N*-methyl-2-pyrrolidone (NMP) [26a]. Free-standing PANI films with an electrical conductivity of 1000 S m^{-1} were examined for EMI SE in the broadband frequency range between 50 MHz and 13.5 GHz. The film with a thickness of 20 μm exhibited approximately 6.1 and 4.6 dB at the two stated frequencies, respectively. As the film thickness increased to 90 μm, the EMI SE value also increased to 18.6 and 17.6 dB at the stated frequencies, respectively. The intrinsic environmental stability of the PANI film resulted in a reliable EMI SE value during a long period. Kumar et al. prepared PANI free-standing film doped with toluenesulfonic acid and 4-chloro-3-methylphenol as first and second dopant, respectively [26b]. The doped PANI films with a thickness of 600 μm exhibited large EMI SE values of 33 and 45 dB from 0.1 to 1000 MHz, which was reliably maintained during a period of three years with little decrease. The PANI film doped by toluenesulfonic acid exhibited greater electrical conductivity and EMI SE compared with the one doped by camphor-10-sulfonic acid. This indicates that the electrical properties of a conducting polymer are directly related to the doping level depending on dopant type. Moreover, the application of PANI was extended into the coating sector based on their advantageous processability. Trivedi and Dhawan prepared a flexible fabric grafted with a PANI layer for EMI shielding application. The product exhibited EMI SE values of approximately 16–18 dB in the range 0.1–1 GHz even though the PANI layer was 1–10 μm thick [30].

Similar to PANI, PPy is an important conducting polymer with good thermal and environmental stability and high electrical conductivity. Unlike PANI, however, the use of PPy as pristine bulk product has limitations of processability because it is generally insoluble in common solvents due to a strong interaction of intra-bonds or inter-bonds in backbone. The as-synthesized PPy has a band gap of 2.5 eV, which facilitates a p-doping process depending on various types of dopants. The intrinsic electrical conductivity of PPY strongly depends on the initial electropolymerization process [31].

Yoshino et al. first reported the EMI SE values of PPy in the range 3–300 MHz [32a]. The PPy was prepared through electrochemical polymerization onto the conducting glass anode with a thickness of 35 μm doped with *p*-toluenesulfonate anion. This doped PPy exhibited a larger electrical conductivity of 2500 S m^{-1} above approximately 30 dB. Kaynak et al. reported EMI SE values of PPy prepared with the same procedure but with different doping level [32b]. The highly-doped PPy with a dopant concentration of 0.060 M exhibited an electrical conductivity of 2300 S m^{-1} and an EMI SE value of 30 dB at 10 GHz, whereas the lightly doped PPy showed an electrical conductivity on the order of 10^{-1} S m^{-1} that highly transmitted the magnetic wave.

Recently, polythiophene (PTP) has also been investigated for electrical conducting applications. PTP with a band gap of 2.0 eV is advantageous based on the chemical diversity through modification of the end-functional group of thiophene molecules. The specific chemical structure of PTP

Table 9.1 Electrical conductivity and EMI SE of typical polymers.

Polymer	Chemical structure	σ (S m^{-1})	SE (dB)	f (GHz)	Reference
PE	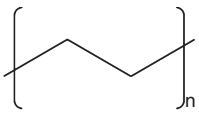	10^{-13}–10^{-17}	<5	8–12	[18]
PS	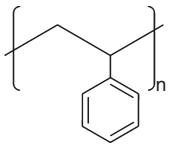	10^{-14}	<1	12–18	[23]
PA(Nylon)	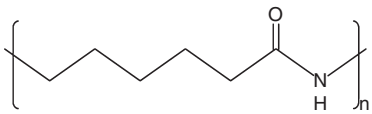	10^{-12}	<0.1	0.3–0.8	[24]
Epoxy (Bisphenol A)	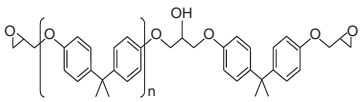	10^{-10}	<3	26–40	[25]
PANI (Emeraldine)	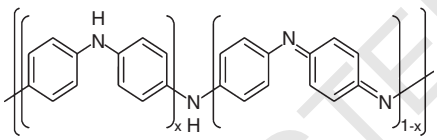	3000–20 000	<45	0.01–13.5	[26]
PPy	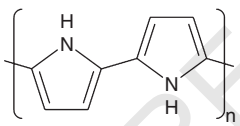	10^{4}–7.5×10^{5}	<30	10	[27]
PTP	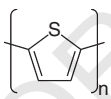	1000–10^{5}	15	2–18	[28]

enables the synthesis of various kinds of chemical derivatives, which provides high solubility, good processability, and increased electrical conductivity. Well-known conducting polymers, such as poly(3-hexylthiophene), poly(3-octylthiophene), and PEDOT, are various derivatives of PTP. Until now, however, only a few results on EMI examinations of pristine PTP derivatives have been reported.

Wu et al. reported the preparation of poly(3,4-ethylenedioxythiophene) (PEDOT) via solid-state polymerization using 2,5-dibromo-3,4-ethylenedioxythiophene (DBEDOT) as monomer for an EMI shielding application in the range 2–18 GHz [28]. The 2 mm thick PEDOT sample exhibited an EMI SE of 15 dB.

As mentioned above, the conducting polymers, also named as synthetic metals, are being recognized as effective EMI shielding materials. However, as shown in Table 9.1, an ICP itself has insufficient EMI SE for real applications; many different kinds of fillers, such as various carbons, magnetic materials, and metallic fillers, need to be incorporated in the ICPs to improve the EMI shielding properties.

9.3 Polymer Composites for EMI Shielding Applications

Polymer composites consist of a polymer matrix with conducting or magnetic fillers. Polymers have many advantages, including their easy processability, low density, low cost, and durable mechanical properties. However, due to their poor and insufficient EMI SE, electrically conducting or magnetically active fillers are incorporated in the polymers to improve their EMI shielding properties.

9.3.1 Carbon Based Filler Materials

Several derivatives of carbon [2, 31] – for instance, graphite, carbon black, carbon nanofibers, carbon nanotubes, and graphene – have extensively been explored as filler materials for EMI shielding applications due to their excellent electrical conductivity, processability, availability, and the ability to provide low percolation thresholds.

9.3.1.1 Graphite

Graphite is a well-known naturally abundant and economical material; therefore, all the initial research on carbon materials focused on graphite for use as carbon filler material in polymer composites. Graphite possesses a layered structure in which carbon sheets are bonded with each other by van der Waals forces to form layers with a high electrical conductivity of 10^3 S cm^{-1} at room temperature [18]. Several approaches for graphite/polymer systems were suggested; however, the aggregation and poor electrical conductivity of the composite product hindered the practical use. Krueger and King [24] reported an EMI SE value of 12 dB at a fairly high graphite content of 25 vol.%. Panwar and Mehra [33] prepared a graphite PE composite that provided a high EMI SE value of 33 dB at a filler content of 18.7 vol.%. Such high filler contents and large thickness motivated researchers to apply novel techniques to improve the percolation threshold and increase the net EMI SE through a decrease in thickness. To achieve this goal, the formation of a segregated structure in polymer composites offered a tremendous opportunity to achieve high values of electrical conductivity and EMI SE even at low conductive filler loadings [34]. Using this approach, Jiang et al. [18] developed a segregated structure interconnecting conductive graphite particles in ultra-high molecular weight polyethylene (UHMWPE) through mechanical mixing the polymer and graphite particles, which were subsequently hot pressed at 200 °C to achieve a compact structure. Figure 9.1 shows the variations of EMI SE values of composites prepared at various filler contents in the range 0.43–7.05 vol.%. With the

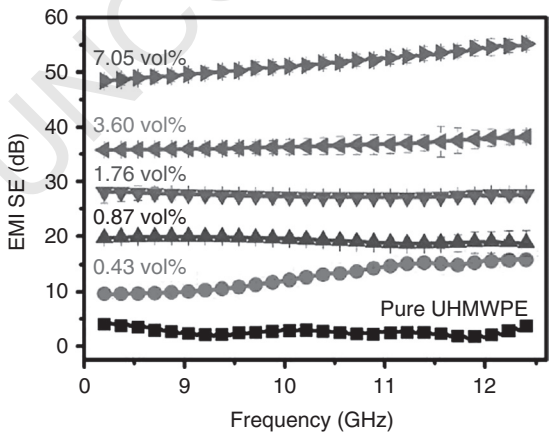

Figure 9.1 Variations of EMI SE values as a function of frequency in the X band for pure UHMWPE and the graphite/UHMWPE segregated composite samples with various graphite contents. *Source:* Reprinted with permission from Ref. [18]. Copyright 2015 Royal Society of Chemistry.

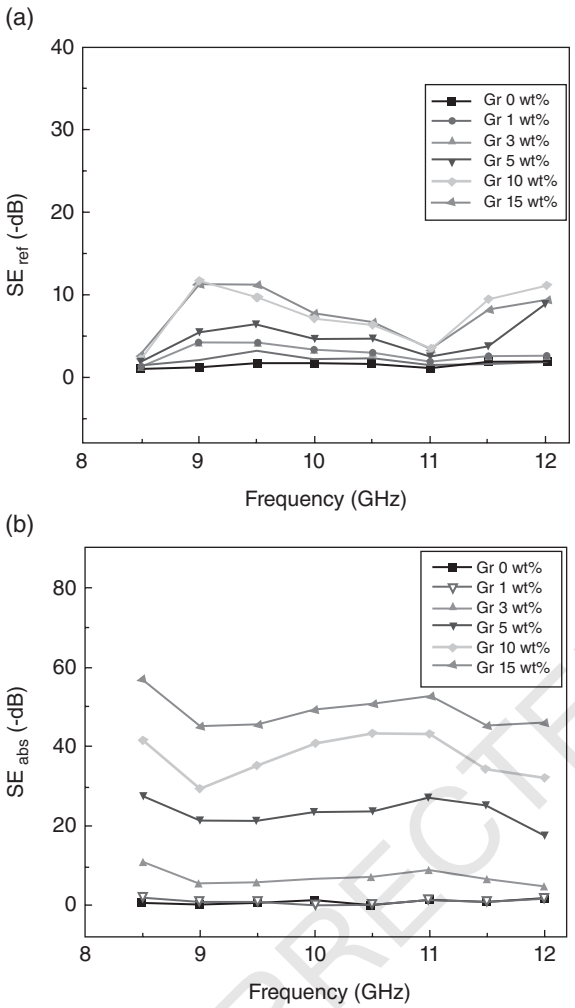

Figure 9.2 Variation of SE as a function of graphite content in graphite/ABS composites at various frequencies for shielding due to: (a) reflection, (b) absorption. *Source:* Reprinted with permission from Reference [35]. Copyright 2011 John Wiley & Sons Inc.

addition of graphite, all the composites showed an increase in EMI SE values compared with the pristine polymer matrix. As the graphite loading increased to 7.05 vol.%, a very high EMI SE value of 51.6 dB was obtained, indicating that only 0.0007% EM wave transmits through the shielding material.

Sachdev et al. [35] developed graphite/acrylonitrile butadiene styrene copolymer (ABS) composites using a tumble mixing procedure at 90–110 °C and 75 MPa. Shielding performance due to reflection and absorption was determined in a frequency range of 8–12 GHz for various graphite loadings in ABS matrix (Figure 9.2). With the increase in graphite content, both the reflection and absorption parts increased, in particular the shielding due to absorption reached a very high value of 60 dB at a thickness of 3 mm for 15 wt% filler loading. The high EMI SE values of graphite/polymer composites are attributed to the excellent conductivity of graphite and the processing method, which results in high EMI SE values at low filler contents.

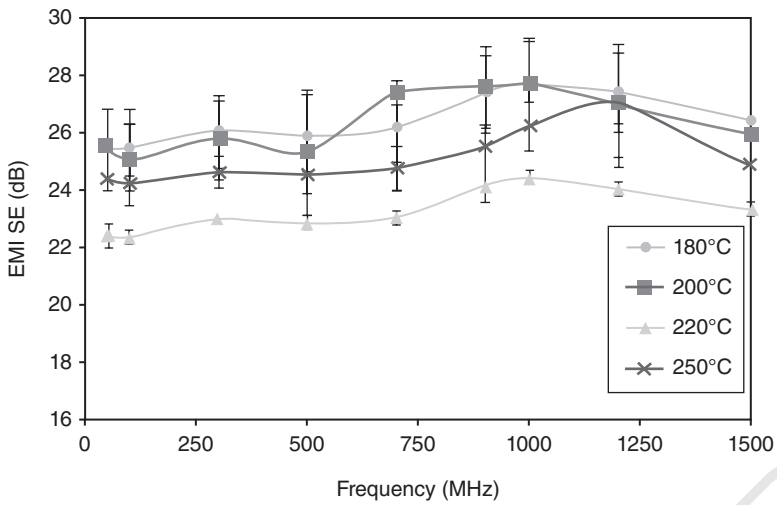

Figure 9.3 Influence of processing conditions on the EMI SE of 7.5 vol.% VGCNF/PS composites. *Source:* Reprinted with permission from Reference [37]. Copyright 2013 Nature Publishing Group.

9.3.1.2 Carbon Fiber

Carbon nanofibers, another derivative of carbon materials, are known for their high electrical conductivity and aspect ratio, giving a peculiar EMI shielding property [36]. Carbon fibers can be synthesized through a vapor grown method, producing great electrical conductivity and aspect ratio at low cost. In one such experiment, Al-Saleh and Sundararaj [37] studied the influence of melt mixing conditions on the level of dispersion and the aspect ratio of vapor grown carbon nanofibers (VGCNFs) in a PS matrix. The processing temperature was varied from 180 to 250 °C to create composites with different microstructures. The effect of processing temperature on the EMI SE of 7.5 vol.% VGCNF/PS composite is depicted in Figure 9.3, revealing an EMI SE value of 24 dB, enough to attenuate 99.6% of the radiation. This level of attenuation is adequate for notebook and desktop computer applications [38].

Foaming of composites is believed to increase the interconnectivity of filler particles and correspondingly increase the electrical and EMI SE properties. Most work has focused on composites made with batch foaming systems and very little attention has been paid to foamed conductive composites made with the injection molding process. In one such experiment, Ameli et al. [39] presented the difference between foamed and solid PP/CF composites with CF content of (0–10 vol.%) using the injection molding process. Foaming reduced the density of the injection-molded PP/CF composites by about 25% and improved their electrical properties. Figure 9.4 shows the variations of EMI SE for the foamed composites as a function of CF content with respect to the total volume of the specimens. It was shown that the final CF content required for the foamed composites to achieve a certain EMI SE values was significantly smaller than that of the corresponding solid ones. In the foamed composites, a final CF content of 6 vol.% was sufficient to achieve an EMI SE value of greater than 20 dB.

9.3.1.3 Carbon Nanotube

Since the discovery of CNTs in the early 1990s, due to their high electrical conductivity and associated EMI SE performance, CNT/polymer composites have attracted great attention, both in academia and industry. The intrinsic high electrical conductivity and aspect ratio enable the realization of polymer composites at low percolation filler loading. Traditionally, CNT composites have been prepared through melt blending or solution mixing techniques. Singh et al. [40]

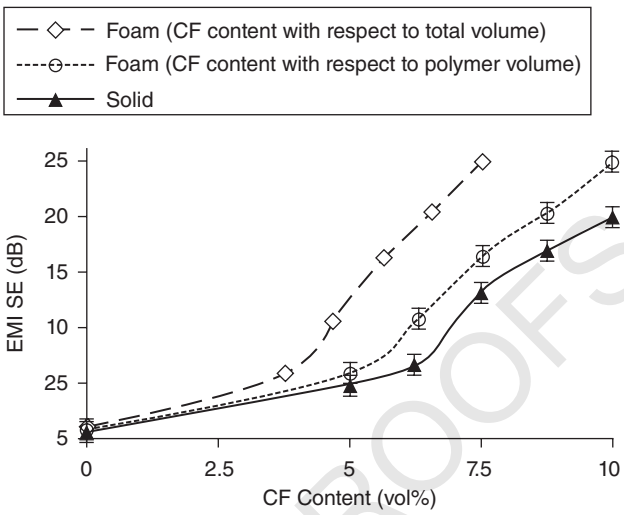

Figure 9.4 Variations of EMI SE for solid and foamed PP/CF composites as a function of CF content. *Source:* Reprinted with permission from Reference [39]. Copyright 2013 Elsevier.

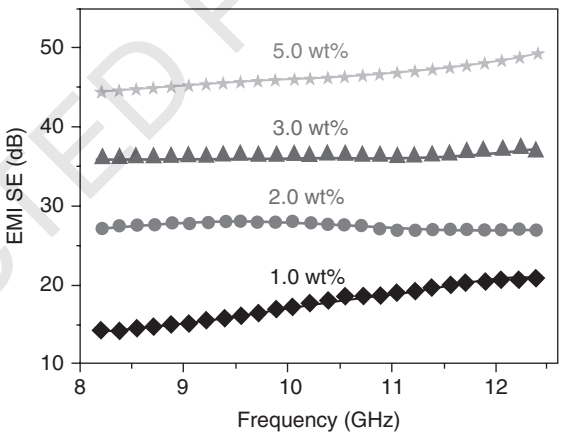

Figure 9.5 Variations of EMI SE of s-CNT/PE composite as a function of CNT content. *Source:* Reprinted with permission from Reference [19]. Copyright 2015 Royal Society of Chemistry.

obtained an EMI SE value of 60.0 dB for a CNT/epoxy composite at a CNT loading of 20.0 wt%. Recently, Jia et al. [19] reported a segregated structure of CNTs in a PE matrix to address the issue of high filler loading. To prepare such segregated structures, generally polymers with a high density character are preferred due to their larger viscosity, which is essential for the elaborate structural design. Figure 9.5 reveals the variations of EMI SE of an s-CNT (segregated carbon nanotube)/PE composite at various filler loadings. Only the composite sample containing 1.0 wt% CNT provided an EMI SE value of 20.8 dB at a frequency of 12.4 GHz, which further increased as the filler loading was increased. The 5.0 wt% CNT content gave an EMI SE of 46.2 dB, which is an exceptionally high value considering the very small filler loading.

In another work, Gupta and Choudhary [41] developed poly(trimethylene terephthalate) (PTT)/multi-walled carbon nanotube (MWCNT) composites through melt compounding at different MWCNT content as an effective lightweight EMI shielding material in the frequency range 12.4–18 GHz Ku-band. The electrical conductivity, permittivity, and EMI SE values of composites were found to depend on the MWCNT content and showed an increase with increasing MWCNT loading. After the percolation limit, the electrical conductivity did not significantly change, whereas the EMI SE increased with increase in loading level (Figure 9.6).

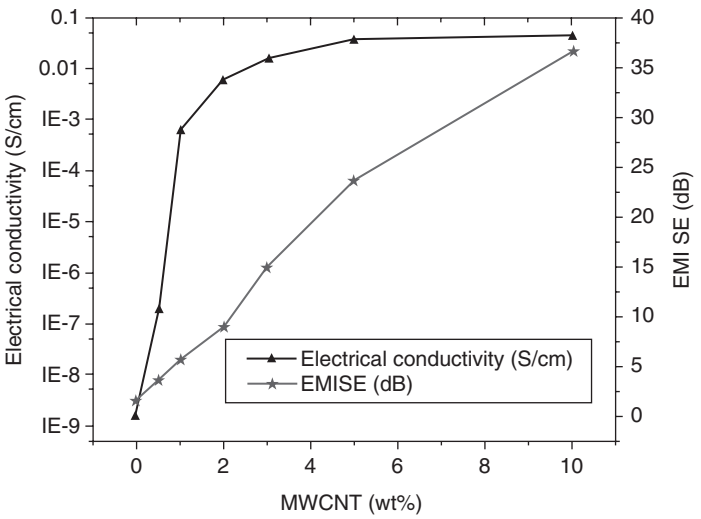

Figure 9.6 Effect of MWCNT content on EMI SE and electrical conductivity (r) of PTT/MWCNT composite. *Source:* Reprinted with permission from Reference [41]. Copyright 2011 Elsevier.

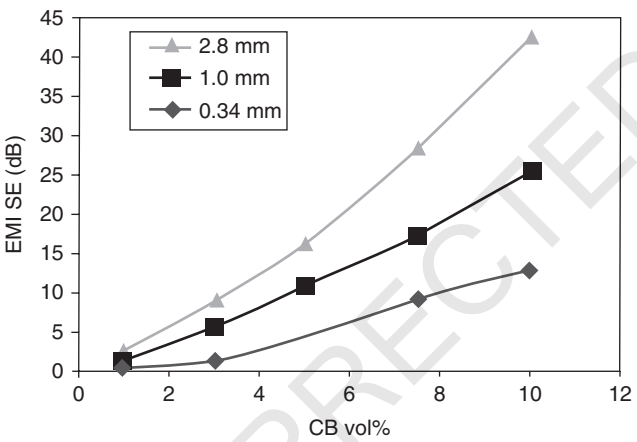

Figure 9.7 Variations of EMI SE of HS-CB/PP composites as a function of filler content and shielding plate thickness in the X-band frequency range. *Source:* Reprinted with permission from Reference [47]. Copyright 2011 IOP Science.

Electrical percolation was achieved at a very small filler content (1 wt%) and EMI SE values of 36–42 dB were recorded for 10 wt% MWCNT loading.

9.3.1.4 Carbon Black

Carbon black (CB) is another carbon product that is easily available and effective for applications requiring high electrical conductivity. The EMI shielding properties of CB/polymer composites have been studied by several researchers [24, 42–45]. Rahaman et al. [43] compared the EMI SE and electrical conductivity of polymer composites utilizing two different types of CBs. They observed that CB with a highly segregated structure exhibited larger electrical conductivity and EMI SE values at the same filler loadings. It can be added to polymer in various forms. Im et al. [46] reported an EMI SE value of 50 dB for 0.5 mm thick samples in the frequency 800 MHz to 4 GHz for carbon composites containing electrospun fibers along with carbon black. A fluorination treatment of CB was also implied to enhance the dispersion of filler in a polymer matrix, resulting in a high electrical conductivity of 3800 S m^{-1} [46]. In another report, Mohammed et al. [47] presented the EMI SE and electrical conductivity properties of high structure carbon black (HS-CB)/PP composites in the X-band frequency range. Figure 9.7

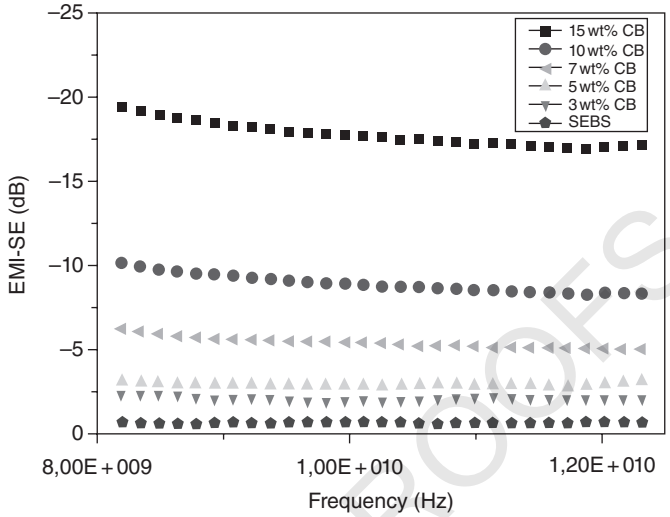

Figure 9.8 Variation of EMI SE for SEBS/CB composites with 3, 5, 7, 10, and 15 wt% of CB. *Source:* Reprinted with permission from Reference [48]. Copyright 2016 Elsevier.

shows the influence of filler content and composite thickness on the EMI SE of HS-CB/PP composites. An increase in EMI SE with increasing filler content and shielding plate thickness was observed. The increase in EMI SE with filler content was ascribed to an enhanced contribution from the reflection and absorption parts of EMI SE, whereas the increase in EMI SE with thickness was largely attributed to increasing contribution from absorption.

Kuester et al. [48] developed electrically conductive poly[styrene-*b*-(ethylene-*ran*-butylene)-*b*-styrene] (SEBS) filled CB through melt blending using a torque rheometer equipped with a mixing chamber. Figure 9.8 exhibits the effect of filler loading on the EMI SE of SEBS composites. EMI SE increased with increasing conductive filler loading, as expected, because the EMI SE values of electrically conducting composites depend on the formation of conducting pathways in the insulating polymer matrix. The largest EMI SE value of 19 dB was recorded at 15 wt% filler content, suggesting the high effectiveness of CB as filler in carbon-based polymer composites.

9.3.1.5 Graphene

Graphene has been a major filler used in various forms in polymer composites. As the EMI SE of a composite material depends mainly on the filler's intrinsic conductivity, dielectric constant, and aspect ratio, it is expected that the use of atomic-thick graphene, with large aspect ratio and high conductivity, would provide a high EMI SE [1, 49–51]. Several papers have reported the use of pristine reduced graphene oxide particles, graphene thin films, and graphene powder in addition to some magnetic fillers. Reduced graphene sheets were also dispersed in electrically conductive polymers [52, 53] in order to improve their shielding properties. Bingqing et al. [22] compared the EMI SE properties of single-wall carbon nanotube (SWCNT) and graphene sheets filled PANI (GS/PANI). The authors revealed that the conductivity and EMI SE of GS/PANI composites are better than those of the SWCNT/PANI composites. Song et al. [54] developed multilayer graphene/polymer composite films with good mechanical flexibility in sandwich-type structures to evaluate their EMI shielding properties. An EMI SE value of up to 27 dB for a mere 0.3 mm thick wax-based sandwich structure was reported, which was enough to shield more than 99% of incident radiation and could serve as a low weight alternative to thick polymer-based composite shields. Liang et al. [49] prepared a composite through dispersion of partially reduced graphene sheets into epoxy resin precursor followed by annealing of the film.

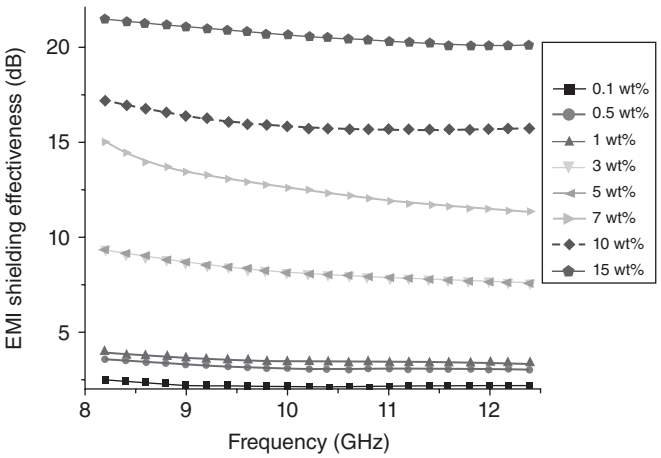

Figure 9.9 Changes of EMI SE for graphene/epoxy composites with various graphene (SPFG) loadings as a function of frequency in the X-band. *Source:* Reprinted with permission from Reference [49]. Copyright 2009 Elsevier.

A low percolation threshold for this composite was obtained at only 0.52 vol.% filler content. Figure 9.9 presents the variations of EMI SE of a graphene/epoxy composite with various filler loadings. The largest EMI SE value of 21 dB in the X band was recorded for 15 wt% graphene loading, indicating that the graphene based polymer composites may be used as lightweight effective EMI shielding materials.

In another paper, Shahzad et al. [23] reported the effects of sulfur doping on improvement of EMI SE for rGO/PS composites. An EMI SE value of 24.5 dB was observed for 7.5 vol.% sulfur-doped rGO loading in a PS matrix, which was 15% larger than for the undoped rGO/PS composites (21.4 dB) at similar filler content. Figure 9.10 shows the effect of filler content on the EMI SE of composites. Shielding due to absorption was more pronounced than that for reflection. This observation was attributed to better conductivity of fillers and the ability to create dielectric losses in the polymer composites. Resultantly, a much shorter skin depth was observed for the doped samples, suggesting the beneficial role of doping in enhancement of the EM properties.

Table 9.2 shows the comparison of EMI SE values along with the effect of filler loading and thickness of various carbon-based polymer composites.

9.3.2 Magnetic Fillers

9.3.2.1 Magnetic Fillers and Carbon Materials in Insulating Polymer Matrix

Several polymer composites containing one or two magnetic constituents in conjunction with carbon materials have been reported for EMI shielding applications using either conducting or insulating polymers as matrix. Common polymers, such as paraffin, epoxy, PVDF, and PVA, have been used extensively as binder in several reports [67–72]. Iron oxide, as the most important magnetic filler, has been explored extensively for microwave absorption properties. A high microwave absorption of −32.5 dB was reported for 15 wt% filler content of rGO/Fe_2O_3 composite to impart conductive and magnetic contributions to paraffin wax, enough to attenuate more than 99.9% of incident radiation [67]. Shen et al. [9] studied the EMI shielding properties of ferroferric oxide (Fe_3O_4)–graphene/polyetherimide (PEI) composite foam and reported a specific EMI SE value of 41.5 dB $cm^3 \cdot g^{-1}$ for composite containing 10 wt% filler. Artificial hybrid films were fabricated using a simple evaporation-induced assembly method consisting of rGO and magnetic graphene (MG) particles with PVA acting as binder [71]. At a very small thickness of 0.36 mm, a reasonable EMI SE (total shielding effectiveness) value of 20.3 dB in the X-band

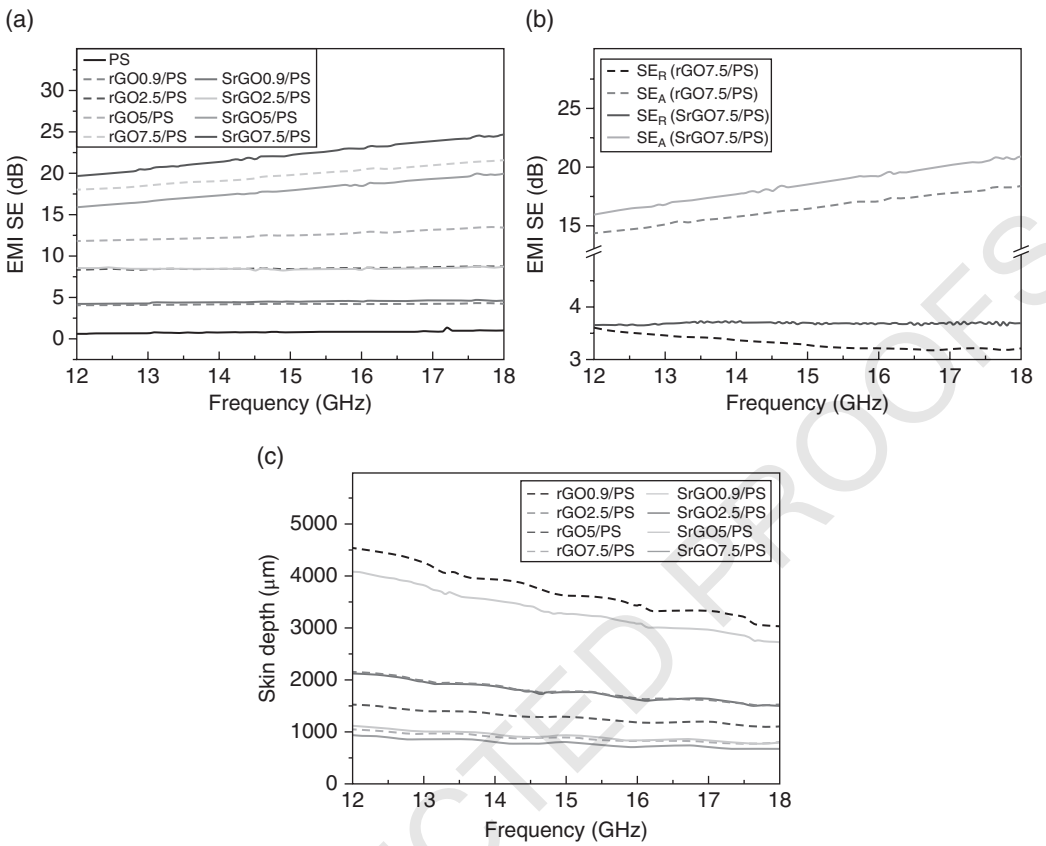

Figure 9.10 (a) EMI SE_T of rGO/PS and SrGO/PS nanocomposites, (b) SE_A and SE_R of rGO7.5/PS and SrGO7.5/PS, and (c) skin depth of rGO/PS and SrGO/PS composites. *Source:* Reprinted with permission from Reference [23]. Copyright 2015 Elsevier.

range was observed (Figure 9.11). Furthermore, the dependence of SE_A and SE_R of hybrid films as a function of frequency was also investigated. The MG hybrid film revealed a greater SE_A than the RGO film, suggesting a better EMI absorption property. In these hybrid films containing magnetic particles, absorption makes a larger contribution to EMI SE than does reflection, supporting the hypothesis that magnetic nanoparticles can enhance EMI properties when used with conductive graphene. Such flexible thin films using PVA are a good option for use in applications where shielding with intricate shapes is required.

Bayat et al. [73] showed the positive influence on EMI SE by addition of Fe_3O_4 in combination with carbon nanofibers (Figure 9.12). The samples were designated with filler contents as 10PAN900, A3F900, and A5F900 containing 0, 3, and 5 wt% Fe_3O_4, respectively. With the increase in filler content both the electrical conductivity and EMI SE values were improved. The good performance was attributed to the increment of both magnetic and dielectric losses due to the incorporation of magnetite nanofiller (Fe_3O_4) in the electrically conducting carbon nanofiber matrix as well as the specific nanofibrous structure of carbon nanofiber mats, which form a higher aspect ratio structure with randomly aligned nanofibers.

Pawar et al. [13] introduced a new approach to tailor the electrical conductivity and EMI SE properties of polymer blends with the addition of graphene and magnetic particles. The EM attenuation capability, in both X and Ku-band frequencies, was assessed in PC (polycarbonate)/

Table 9.2 EMI SE values of carbon-based polymer composites.

Matrix/filler	Preparation method	Filler (%)	*t* (mm)	σ (S m^{-1})	SE (dB)	*f* (GHz)	Reference
PE/Graphite	Mechanical mixing	7.05 vol.%	2.5	10	51.6	8.2–12.4	[18]
PE/Graphite	Mechanical mixing	18.7 vol.%	3	—	33	8.2–12.4	[33]
PA 6,6/Graphite	Mechanical mixing	25 vol.%	3.2	—	12	0.2–1.2	[24]
PU/Graphite	In situ	6.5 vol.%	1	10	19.3	0.9–1	[55]
ABS/Graphite	Mechanical mixing	15 wt%	3	16	60	8.2–12.4	[35]
Epoxy/Graphite	Solution Mixing	2 wt%	5	2.6	11	8–18	[56]
PDMS/CB/CNF	Electrospinning	—	—	38	50	0.8–4	[46]
SEBS/CB	Melt blending	15 wt%	5	22	20	8.0–12.0	[48]
PS/CNF	Melt mixing	7.5 vol.%	2	—	22–26	0.1–1.5	[37]
PP/CF	Melt mixing	10 vol.%	3.2	10	25	8.2–12.4	[39]
Epoxy/CNT	Solution Mixing	0.5 wt%	5	2	9	8–18	[56]
PTT/MWCNT	Melt mixing	10 wt%	2	80	36–42	12.4–18	[41]
PS/G–MWCNT	In-situ solution mixing	3.5 wt%	5.6	—	20.2	8.2–12.4	[57]
PS/MWCNT	Solution mixing	20 wt%	2	1	63	8.2–12.4	[58]
PS/CNT	Solution mixing	7 wt%	—	5×10^{-3}	~20	8.2–12.4	[59]
PE/CNT	Mechanical mixing	5 wt%	2.1	80	46.4	8.2–12.4	[19]
Epoxy/SPFG	In situ	15 wt%	—	—	21	8.2–12.4	[49]
PS/FGS	Solution mixing	30 wt%	2.5	1.25	29.3	8.2–12.4	[60]
PS/SrGO	Solution mixing	7.5 vol.%	2	33	24.5	12–18	[23]
PS/rGO	Solution mixing	3.47 vol.%	2.5	—	48	8.2–12.4	[61]
PE/rGO	In-situ	1.5 wt%	2.5	3.4	32.4	8.2–12.4	[62]
PMMA/rGO	Solution mixing	4.23 vol.%	3.4	10	30	8.2–12.4	[63]
PMMA/rGO	Solution mixing	1.8 vol.%	2.4	3.1	13–19	8.2–12.4	[64]
PEI/rGO	Solution mixing	5.87 vol.%	2.3	4.8×10^{-6}	20	8.2–12.4	[65]
PDMS/graphene	CVD	0.7 wt%	2.5	1800	30	0.03–1.5	[66]
PS/SrGO	Solution mixing	7.5 vol.%	2	33	24.5	12–18	[23]

SAN (styrene acrylonitrile copolymer) (60/40, w/w) polymer blends in the presence of graphene and nickel decorated graphene (G–Ni) nanoparticles, as shown in Figure 9.13. The blends with 1 wt% graphene loading manifested an SE value of –6.6 dB, whereas significantly greater SE was observed with increasing graphene loading. The blends with G–Ni showed an extraordinary improvement in EMI SE over blends with graphene. This improvement was due to the fact that G–Ni nanoparticles were well dispersed in the matrix, leading to the attenuation of EM radiation. An SE value of –29.4 dB was recorded for blends with 3 wt% G–Ni, which is significantly larger than that of blends with 3 wt% graphene (–13.7 dB) at 18 GHz frequency.

9.3.2.2 Magnetic Fillers with Carbon Materials in Conducting Polymer Matrix

To further enhance the EMI SE of polymer composites, the use of conducting polymers, such as PANI, PPy, and PEDOT has been reported by several researchers [10–12, 53, 74–81]. Apart from incorporation of magnetic iron oxide as filler, the use of Mn [11, 79] and Zn [12] ferrites

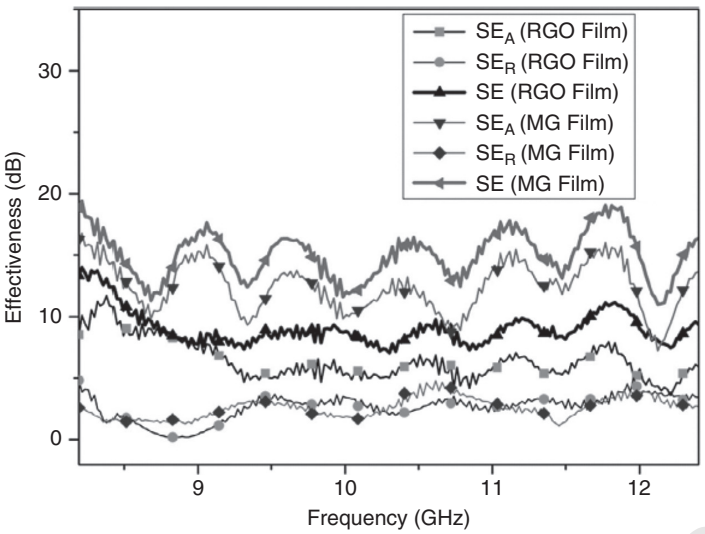

Figure 9.11 Variations of EMI SE_A and SE_R of RGO and magnetic graphene hybrid films with a thickness of 0.23 mm as a function of frequency. *Source:* Reprinted with permission from Reference [71]. Copyright 2014 Elsevier.

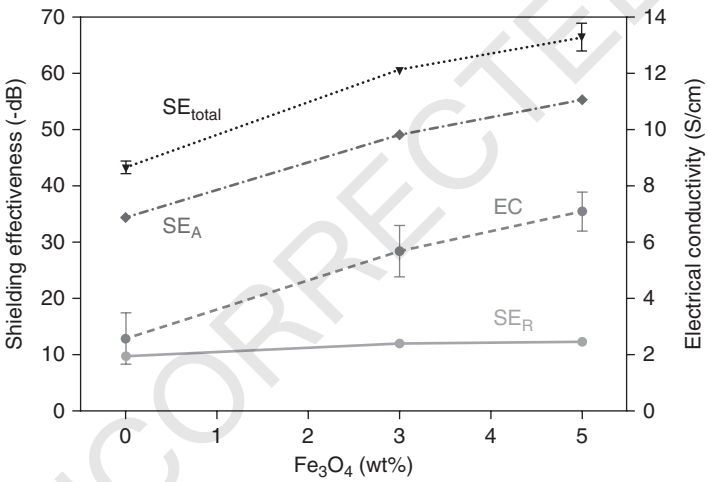

Figure 9.12 Comparison of SE_{total}, SE_A and SE_R at 10.4 GHz for samples 10PAN900, A3F900, and A5F900 containing 0, 3, and 5 wt% Fe_3O_4, respectively (all samples were approximately 0.7 mm thick). *Source:* Reprinted with permission from Reference [73]. Copyright 2014 Elsevier.

has also been reported. Likewise, the use of carbon materials along with magnetic fillers has been observed as a successful approach to address EMI problems [53, 74, 76, 78]. In one such work utilizing the conducting polymer composites along with carbon derivatives and magnetic nanoparticles, Singh et al. [74] develop a 3D nanostructure consisting of chemically modified graphene/Fe_3O_4 (GF) incorporated in PANI. Figure 9.14 presents the shielding contribution due to absorption and reflection with frequency for the different ratios of aniline and graphene. The sample designation followed the pattern: aniline : GF of 1 : 1 (PGF1), aniline : GF of 1 : 2 (PGF2), and aniline : Fe_3O_4 of 1 : 2 (PF12). Interestingly, the PGF composites manifested better

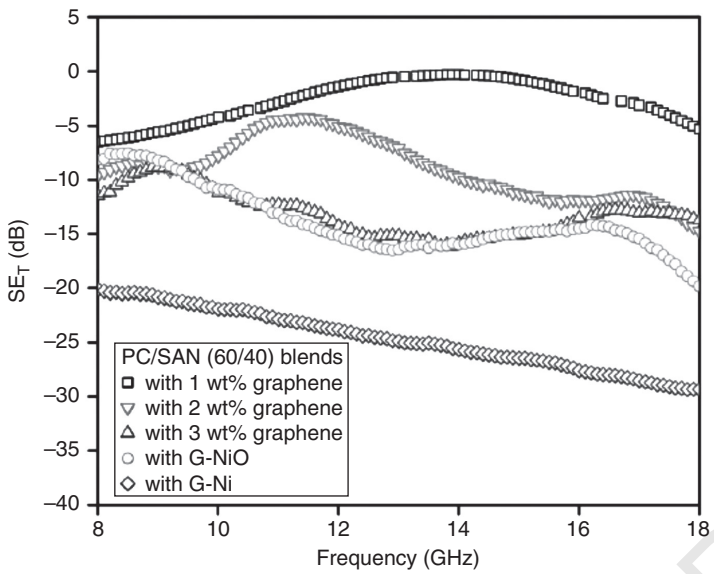

Figure 9.13 Total shielding effectiveness as a function of frequency for PC/SAN blends in the X and Ku-band frequencies. *Source:* Reprinted with permission from Reference [13]. Copyright 2015 Royal Society of Chemistry.

absorption characteristic rather than reflection and showed excellent frequency stability in the measured frequency range, which increased with increasing GF content. The PGF2 sample revealed larger values of SE_A (22–26 dB) and SE_R (4.7–6.3 dB) as compared with values for PGF1 (SE_A = 21 dB and SE_R = 4.5 dB) in the frequency range 12.4–18 GHz. However, PANI–Fe_3O_4 (PF12) exhibited a smaller value of SE (SE_A = 7–9 dB and SE_R = 1.5–2.5 dB) in comparison with PGF series composites at the same frequency range with a specimen thickness of 2.5 mm. This increase in absorption with the addition of magnetic graphene hybrid mainly arises due to the synergistic effect of graphene and Fe_3O_4 with PANI, resulting in greater dielectric and magnetic losses, which are responsible for the overall increase in EMI SE value.

Tung et al. [53] reported Fe_3O_4 with functionalized graphene in PEDOT prepared through poly(ionic liquid) (PIL)-mediated hybridization. Figure 9.15 reveals the variations of EMI SE values for PEDOT-PIL and Fe_3O_4-RGO/PIL-PEDOT composite films with a thickness of 10 μm in the frequency range 20–1000 MHz. At 1 wt% of Fe_3O_4-RGO content, the EMI SE value of the Fe_3O_4-RGO/PIL-PEDOT composite was about 22 dB, which is larger than that of PEDOT-PIL (16 dB). This observation suggests the importance of magnetic particles in the enhancement of microwave absorption properties of polymer.

9.3.2.3 All-Magnetic Fillers in Insulating Polymer Matrix

The use of all-magnetic filler, such as ferrites [82], iron oxides, and other metal oxides [72], is also popular for EMI shielding materials as the wave absorbing property has a direct relationship with the EM characteristic of the absorbants. Guan et al. [72] used manganese dioxide nanoparticles owing to their dielectric loss and resultant good EM wave attenuation property, which are attributed mainly to a flaky and strip-shaped surface topography and to their high multi-reflection and scattering cross-sectional areas. With the increase of MnO_2 content, as shown in Figure 9.16, the reflectivity also increased and the peak values drifted to the lower frequency band, except for the sample in Figure 9.16d. For example, sample 1 (Figure 9.16a) has only one peak value of −11.02 dB at 11.75 GHz, but that of sample 2 (Figure 9.16b) drifted to

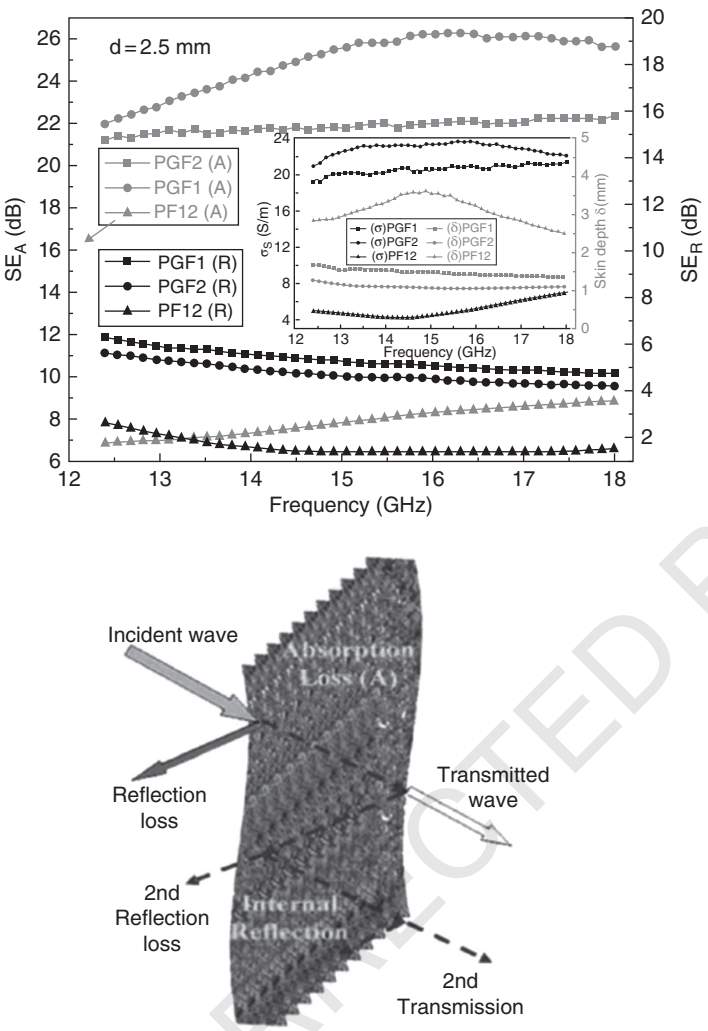

Figure 9.14 Dependence of shielding effectiveness (SE_A and SE_R) of PF12, PGF1, and PGF2 composites as a function of frequency for sample thickness of 2.5 mm; a representation of the EMI SE is also shown. *Source:* Reprinted with permission from Reference [74]. Copyright 2013 Royal Society of Chemistry.

10.43 GHz with the value of −15.17 dB. Samples 3 and 4 shifted their peaks to 8.43 and 8.96 GHz and the reflectivity peak values increased to −24.73 and −18.92 dB, respectively. The decrease in the reflectivity and attenuation peak value of sample 4 (Figure 9.16d) was ascribed to the fact that further increasing concentration of MnO_2 leads to an increase in the amount and the size of MnO_2 contacting aggregates, which degrades the attenuation property of the composite.

Zhu et al. [83] investigated the effects of core–shell structured nanoparticles on the microwave absorption property of polymer composites. The insulating silica (SiO_2) layer on the magnetic particle surface helps to improve the resistivity of the polymer nanocomposites besides decreasing the eddy current losses and increasing the anisotropy energy, which are essentially important to acquire a high EM wave absorption as reflection loss (RL) and broad absorption bandwidth. Polyurethane (PU) nanocomposites filled with Fe@FeO and Fe@SiO_2 nanoparticles

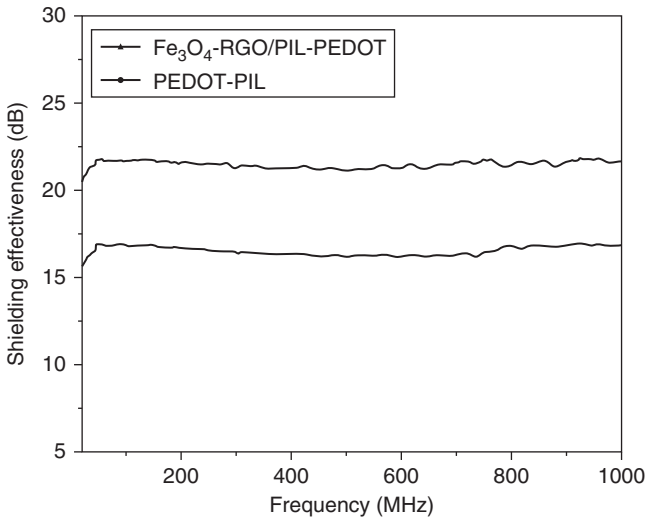

Figure 9.15 Variations of SE of composites containing 1 wt% Fe_3O_4–RGO (upper line) compared with that of pristine PEDOT-PIL (bottom line). *Source:* Reprinted with permission from Reference [53]. Copyright 2012 John Wiley & Sons.

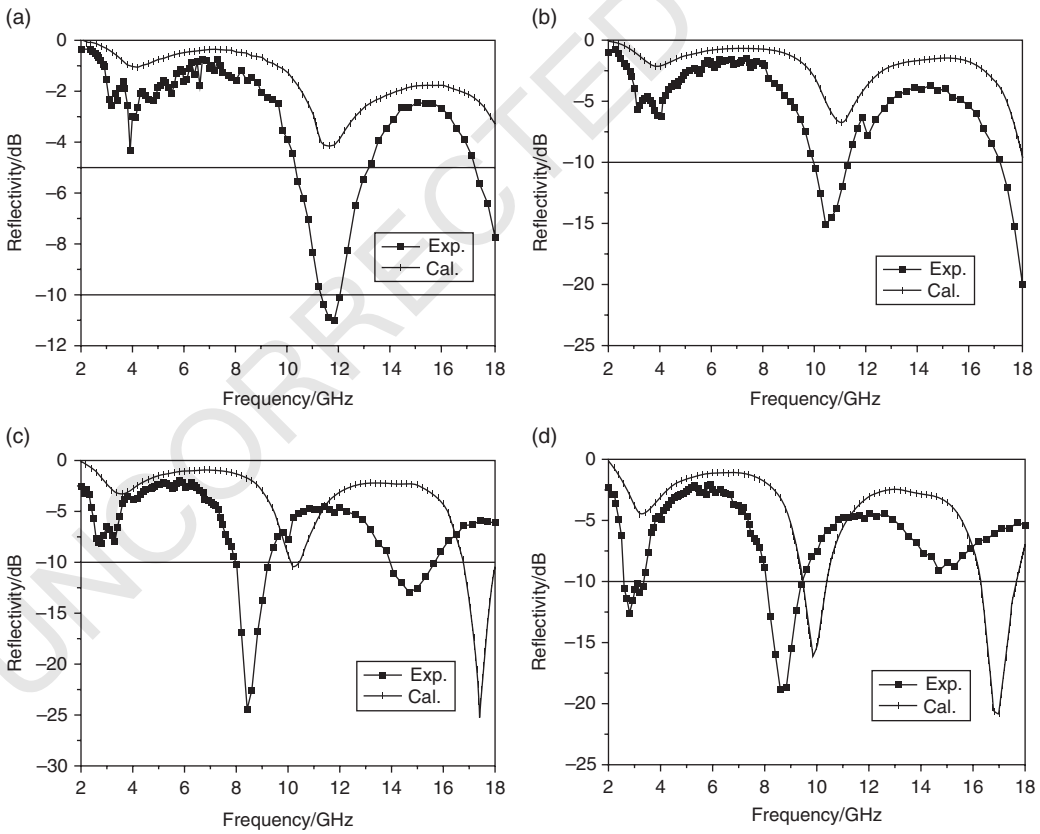

Figure 9.16 Calculated and experimental microwave reflectivity of composites containing various amounts of MnO_2: (a) 10, (b) 20, (c) 30, and (d) 40 vol.%. *Source:* Reprinted with permission from Reference [72]. Copyright 2015 Springer.

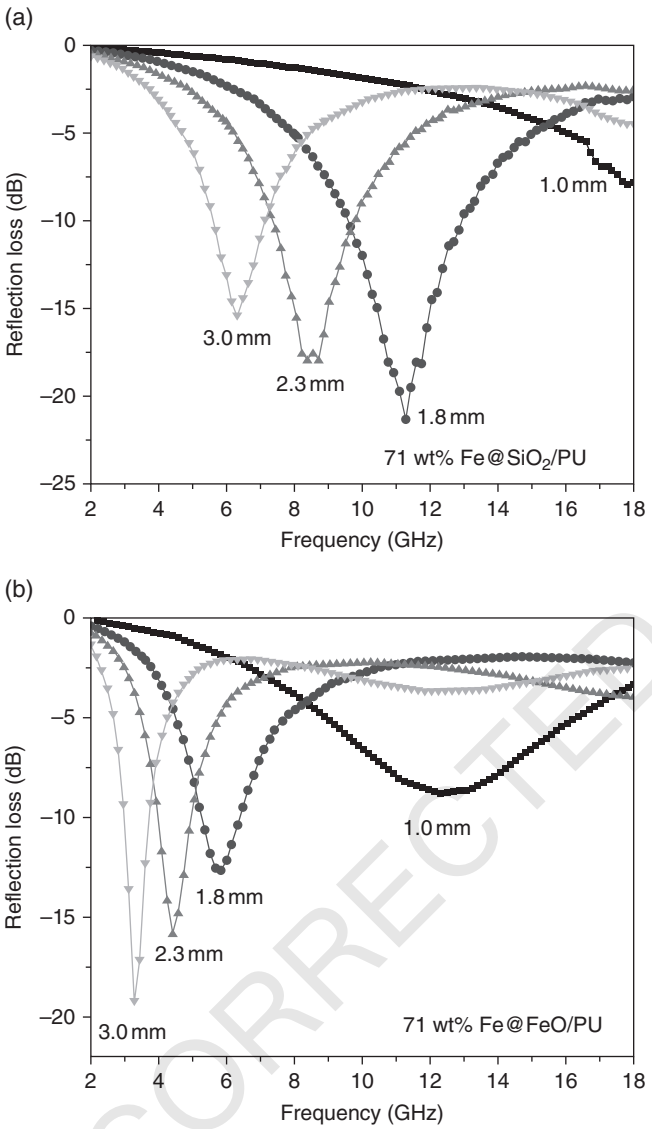

Figure 9.17 Dependence of RL on thickness of absorption layer within the frequency range 2–18 GHz: (a) 71 wt% Fe@SiO_2/PU and (b) 71 wt% Fe@FeO/PU PNCs. *Source:* Reprinted with permission from Reference [83]. Copyright 2011 American Chemical Society.

were fabricated via a surface-initiated polymerization (SIP) method. Figure 9.17 shows the calculated RL of both the Fe@SiO_2/PU and the Fe@FeO/PU composites with the sample thickness varied from 1 to 3 mm. The minimum value of RL reached was −21.2 dB at 11.3 GHz for the Fe@SiO_2/PU sample with a thickness of 1.8 mm (Figure 9.17a). Furthermore, the absorption bandwidth with an RL value below −10 dB was up to 7.5 GHz, whereas for the Fe@FeO/PU composite the absorption bandwidth of RL below −10 dB was only 3.4 GHz and the minimum RL value was not able to reach −20 dB even when the absorber thickness was increased to 3 mm (Figure 9.17b). The Fe@SiO_2/PU composites showed the minimum RL value, a broader absorption bandwidth, and a smaller absorber thickness, indicating that the silica shell plays a positive

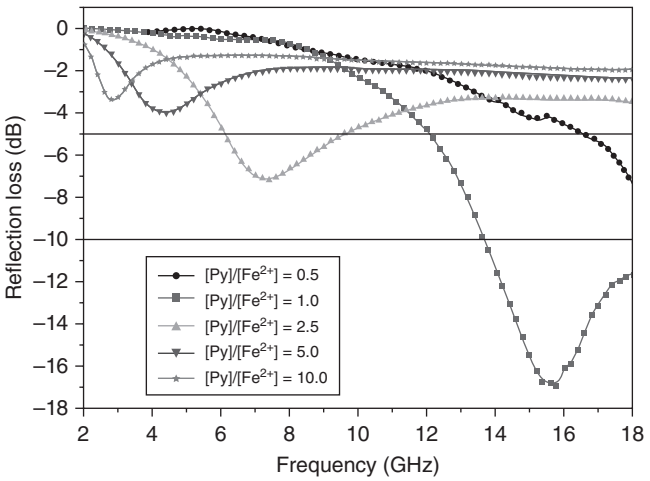

Figure 9.18 Variation of reflection loss (RL) with frequency for α-FeOOH nanorods/PPy composites at different [Py]/[Fe2+] ratios (specimen thickness = 2 mm). *Source:* Reprinted with permission from Reference [80]. Copyright 2010 Elsevier.

role in the microwave absorption properties of $Fe@SiO_2$/PU nanocomposites, which are poised to be very promising for new types of EM wave absorptive materials.

9.3.2.4 All-Magnetic Fillers in Conducting Polymer Matrix

Similar to composites of all-magnetic nanofillers in an insulating polymer matrix, research results on the possibility for using conducting polymer matrixes have been reported. Xu et al. synthesized barium ferrite/PPy nanocomposites [10] and nickel/PPy core–shell nanocomposites [84]. The authors found that the nanocomposites provide better RL properties than when only barium ferrite or nickel are used. Similarly, Li et al. [12] reported that the $ZnFe_2O_4$/PPy core–shell nanocomposites exhibit much better microwave absorption performance than $ZnFe_2O_4$ alone. Xiao et al. [80] reported the in-situ formation of α-FeOOH nanorods in a PPy matrix. The PPy nanocomposites exhibited good conductivity and antiferromagnetic behavior. The calculated results for the RL value based on the absorbing wall theory showed that the PPy nanocomposite with a $[Py]/[Fe^{2+}]$ of 1.0 provides the best microwave absorption in the frequency range 2–18 GHz. Figure 9.18 exhibits the results for RL measurements of composite as a function of frequency at a fixed thickness of 2 mm. It was observed that the frequency for the minimum RL value decreases with increasing the $[Py]/[Fe^{2+}]$ ratio. The minimum RL values obtained for the specimens with the ratios $[Py]/[Fe^{2+}]$ of 1.0 and 2.5 were – 15.8 dB at 15.8 GHz and – 7.16 dB at 7.4 GHz, respectively. Here, the sample with ratio $[Py]/[Fe^{2+}]$ of 10, despite having high electrical conductivity, revealed smaller microwave absorption properties. It was proposed that the microwave absorbing parameters of the conducting polymers, such as PPy, are not directly proportional to the electrical conductivity [84, 85]. The one-step synthesis for making PPy composites and competitive price of α-FeOOH nanorods make the nanocomposites feasible as microwave absorbing materials for practical applications.

In another similar polymer system, Singh et al. [81] reported the preparation of PEDOT ferri-magnetic conducting polymer composites through incorporation of magnetic particles. The synthesis of PEDOT–g-Fe_2O_3 composite was carried out via chemical oxidative polymerization of EDOT with ferrite particles in the presence of dodecylbenzenesulfonic acid (DBSA), which works as dopant and as surfactant in aqueous medium. Figure 9.19 shows the variations of EMI SE values for PEDOT–DBSA and PEDOT–g-Fe_2O_3 composite in the frequency range 12.4–18 GHz. The calculated SE_R and SE_A values for PEDOT–DBSA were 1.63 and 8.41 dB at 15.2 GHz, whereas in the case of PEDOT–g-Fe_2O_3 composite the SE_R and SE_A values were

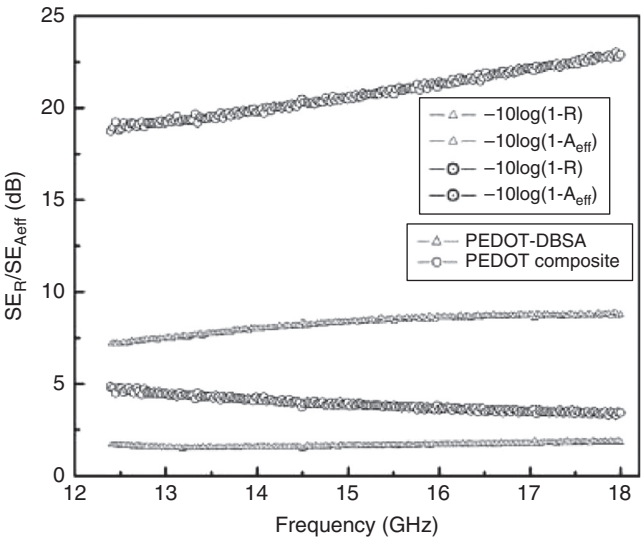

Figure 9.19 Variation of SE due to absorption (SE_{Aeff}) and reflection (SE_R) with frequency in the P-band (12.4–18 GHz) of PEDOT–DBSA and PEDOT–ferrite composite. *Source:* Reprinted with permission from Reference [81]. Copyright 2008 John Wiley & Sons.

obtained as 3.82 and 20.7 dB, respectively. The PEDOT–g-Fe_2O_3 composite also possesses good saturation magnetization (M_s) value of 20.56 emu g^{-1} and a conductivity of 0.4 S cm^{-1}, which means it can find applications as an innovative microwave absorbing material.

Table 9.3 compares the EMI SE of different polymer composites embedded with magnetic and carbon fillers. The effect of filler content and thickness is presented (where available) along with the preparation methods for making polymer composites.

9.3.3 Metal-Based Filler Materials

Metals are excellent conductors of electricity and can reflect, absorb, and transmit EM waves [2]. Traditionally, metals were used in the form of thin films or coating on polymer substrates. With the passage of time and due to a few limitations, such as corrosion, the focus was shifted to use metals in the form of nanoparticles or fibers in the polymer matrices. Metals with a small unit size are believed to be more effective than metals a large one, though a small unit size is not convenient to disperse in a matrix. Several metals have been used as filler in polymer matrices to make composite materials for EMI shielding applications. For instance, metals with high electrical conductivity and availability, such as aluminum, nickel, silver, and iron, have been explored the most.

Aluminum is relatively inexpensive, but it is easily oxidized in air. The oxide layer on the aluminum surface causes a reduction in electrical conductivity. Aluminum fibers on the other hand may be advantageous due to their ability to reach the percolation limit at smaller filler contents. However, aluminum fibers are difficult to compound with polymers owing to aggregation during processing. Nickel is another metal frequently used in polymer composites for EMI shielding on account of its high electrical conductivity. However, nickel has a relatively high density and its processing is difficult; thus, researchers have investigated its composites [99–103] with different polymer matrices. For example, Gargama et al. studied the electromagnetic properties of PVDF/Ni composites prepared at various compositions (f_{con}) using a mortar and pestle [102]. The resultant composites revealed large dielectric constants around the percolation threshold (f_c), which is a typical feature of metal fillers. The EMI SE value of the composites increased from 11 to 23 dB when the filler volume fraction was increased from 0.2 to 0.4, respectively

Table 9.3 EMI SE values of magnetic particle filled along carbon materials in polymer matrix.

Matrix/filler	Preparation method	Filler content	*t* (mm)	σ (S m^{-1})	(Ms) emu·g^{-1}	SE (dB)	Max RL (dB)	*f* (GHz)	Reference
Paraffin/rGO-Fe_2O_3	Solution mixing	15 wt%	3	—	—	—	−32.5	2–18	[67]
Paraffin/RGO/γ-Fe_2O_3	Solution mixing	45 wt%	2.5	1.8×10^{-5}	—	—	−59.6	10	[68]
Wax/rGO/Fe_3O_4@Fe/ZnO	Solution mixing	20 wt%	5	—	13.8	—	−30	2–18	[69]
Paraffin/Fe_3O_4/MWCNT	Solution mixing	—	3	—	31.4	—	−75	2–18	[70]
PVA/rGO/Fe_2O_3	Solution mixing	—	0.36	—	5.2	20.3	—	8.2–12.4	[71]
PVA/MnO_2/SiO_2	Mechanical mixing	30 vol.%	8	—	—	—	−25	2–18	[72]
PVDF/rGO/Fe_2O_3	Solution mixing	5 wt%	2	—	—	—	−43.97	2–18	[86]
PVDF/Ni-Ferrite	Solid state	—	2	—	—	67	—	8.2–12.4	[82]
PVDF/RGO/$MnFe_2O_4$	Solution mixing	5 wt%	3	—	44.2	—	−29	2–18	[87]
PVDF/rGO/Co_3O_4	Solution mixing	10 wt%	4	—	—	—	−25.05	2–18	[88]
PP/ash/ Fe_2O_3	In situ	60%	2	1	13.55	25.5	—	12.4–18	[89]
PS/rGO/ Fe_3O_4	Solution mixing	2.2 vol.%	—	21	81	30	—	9.8–12	[90]
Epoxy/CNF/ Fe_3O_4	Solution mixing	10 wt%	13	0.2	—	20	—	1–18	[91]
PU/ Fe@SiO_2 nanoparticles	Solution mixing	71 wt%	2	—	137	—	−20	2–18	[83]
PDMS/Fe_3O_4/CNF	Solution mixing	5 wt%	0.7	—	—	67.9	—	8.2–12.4	[73]
PAN/Fe_3O_4/CNF	Electrospinning	2 wt%	2	120	13.53	—	−45	2–18	[92]
PVC/rGO/Fe_3O_4	Solution mixing	10 wt%	1.8	7.7×10^{-4}	12	13	—	8–12	[93]
PEO/rGO	Solution mixing	2.6 vol.%	2	—	—	—	−38.8	2–18	[94]
PEI/rGO/Fe_3O_4	Phase separation	10 wt%	2.5	10^{-4}	3.09	14–18	—	8–12	[9]
SDS/rGO/Fe_2O_3	Solution mixing	>85 wt%	—	—	12	33	—	12.4–18	[95]
PC/SAN/rGO/Ni	Solution mixing	>4 wt%	1.5	—	28	−29.4	—	8–18	[13]
PANi/rGO/Fe_3O_4	In situ	—	2.5	260	—	26	—	12–18	[74]
PANi/ Fe_2O_3/TiO_2	In situ	—	—	—	—	—	−45	8.2–12.4	[75]
PANi/CIP/Fe_3O_4	Mechanical mixing	—	1.76	—	123	—	−48.3	9.6	[76]

PANi/Fe_3O_4	In situ	40 wt%	2	—	—	—	−33.5	2–18	[77]
PANi/rGO/Fe_2O_3	In situ	60%	2.5	5383	2.47	51	—	8.2–12.4	[78]
PANi/$MnFe_2O_4$	In situ	15 wt%	1.4	—	1.59	—	−15.3	8–12	[11]
PANI/rGO/Ni	In situ	—	3.5	—	20.8	—	−51.3	2–18	[96]
PPY/ $MnFe_2O_4$	In situ	15 wt%	1.5	—	10	—	−12	8–12	[79]
PPY/α-FeOOH	In situ	30 wt%	2	1610	4.8	—	−17	2–18	[80]
PPY/$BaFe_{12}O_{19}$ in wax	In situ	38.2 wt%	2	>1	2.5	—	12	2–18	[10]
PPY core–shell $ZnFe_2O_4$ in paraffin	In situ	50 wt%	2.7	—	17.8	—	−28.9	2–18	[12]
PPY/CIP	In situ	50 wt%	2.2	—	—	—	−39.5	2–18	[97]
PEDOT/ Fe_2O_3	In situ	—	6	40	20.56	22.8	—	12.4–18	[81]
PEDOT/rGO/Fe_3O_4	Solution mixing	1 wt%	0.01	—	0.19	22	—	0.02–1	[53]
PEDOT/Ba ferrite	In situ	—	—	—	—	22.5	—	12.4–18	[98]

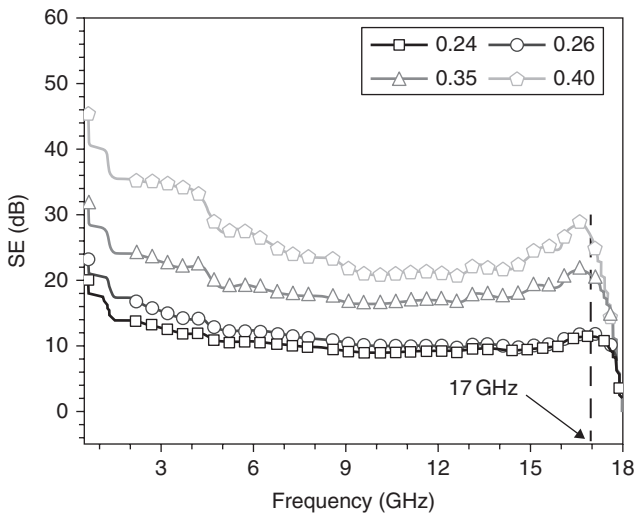

Figure 9.20 Shielding effectiveness of PVDF/Ni composites. *Source:* Reprinted with permission from Reference [102]. Copyright 2015 AIP Publishing.

(Figure 9.20). Nickel was also used with carbon fillers, such as carbon nanotubes and carbon black, or as coating material on the conductive fillers [100, 101]. Metal/carbon hybrid fillers have certain advantages; for instance, they can achieve high electrical conductivity and dielectric constant. Some metals, including nickel, enhance magnetic permeability, which is a key parameter in terms of absorbing EM energy.

Silver, another versatile element, has the greatest electrical and thermal conductivities among all metals [104]. These unique properties make silver useful for commercial applications; however, the cost factor limits its use in some applications. Several researchers have investigated silver nanocomposites in the forms of particles, wires, and plating materials [104–107]. Li et al. investigated Ag-plated carbon fiber (APCF)/epoxy composites. As the filler content in the composite increased to 7 wt%, the volume and surface resistivity decreased [106]. Composite with 4.5 wt% filler content exhibited SE values of 38–35 dB at the X-band range (8.2–12.4 GHz) (Figure 9.21a). The thermal conductivity of composite was also improved, which is approximately 2.5 times larger than that of CF/epoxy composites with the same composition. The authors suggested that heat can transfer along the interconnected network in the composites. It was also observed that APCF dramatically enhances both impact and flexural strengths (Figure 9.21b).

Recently, Kim et al. investigated EMI SE-transparent and flexible silver nanowire/polyimide composites using plasma treated and electroless Cu plated nanowires [105]. The value of EMI SE for Cu/AgNWs/PI film was obtained as 55 dB at specimen thickness of smaller than 10 μm (Figure 9.22), being thought suitable for various electronic devices that require transparency and flexibility.

Copper is a ductile and highly electrical and thermal conductive metal. Because of its good electrical properties and low cost, copper is widely used in electronics. However, the oxidation of copper considerably degrades its electrical properties. Researchers have studied copper composites to prevent this drawback and have realized great EMI SE values using several techniques [108–110].

To summarize, metals are excellent candidates for shielding EM waves. They have high electrical conductivity, dielectric constant, and some degrees of permeability. Extensive research has been conducted to improve the drawbacks of metal, trying to produce lightweight, easily processable, and highly EMI shielding composites. Table 9.4 shows different metal-filled polymer composites along with their EMI SE values.

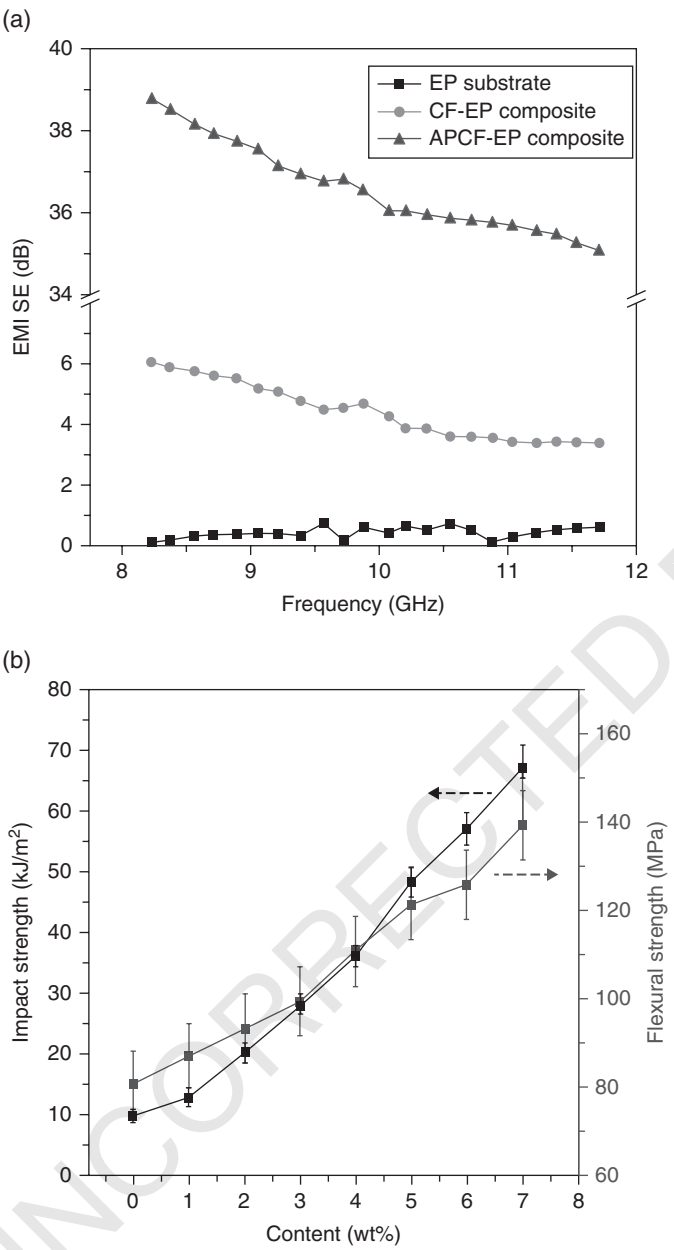

Figure 9.21 Properties of APCF/epoxy composites: (a) EMI SE and (b) mechanical strength. *Source:* Adapted with permission from Reference [106]. Copyright 2015 John Wiley & Sons.

9.4 Structured Polymer Composites for EMI Shielding

Various structured composites, such as foam, sandwich, and segregated structures, have been investigated for high performance EMI SE. The main purpose was to reduce the weight and increase the flexibility of the composite materials while keeping acceptable shielding properties. Indeed, the structured materials can improve the specific values of EMI SE, which is beneficial

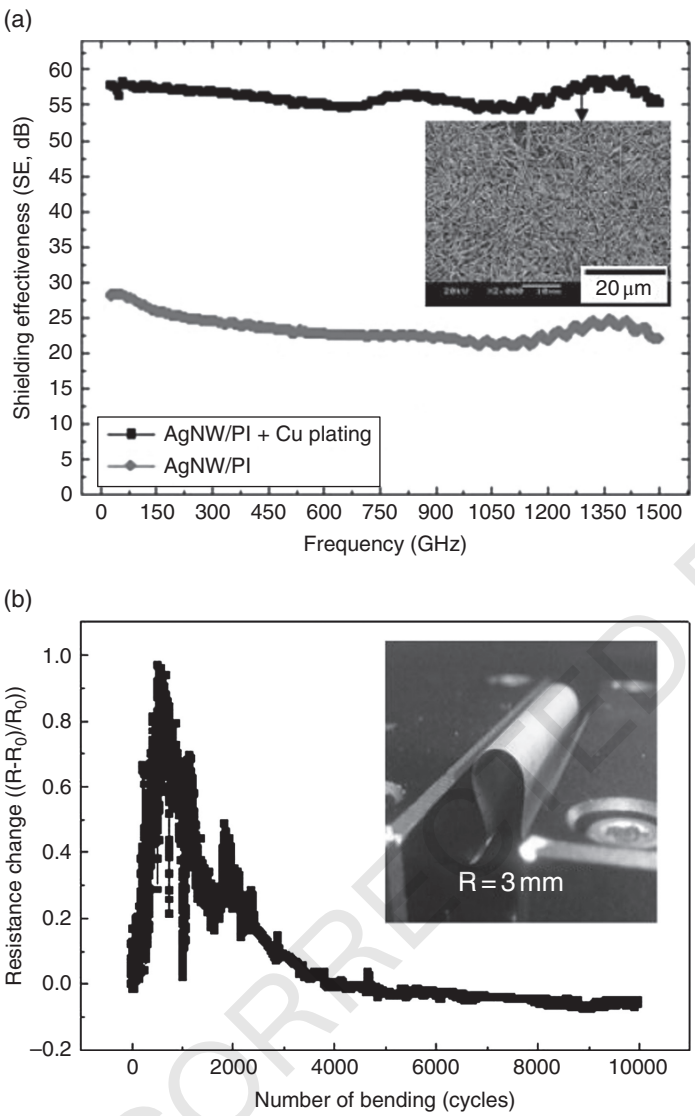

Figure 9.22 Properties of a Cu/AgNWS/PI film: (a) Variations of SE up to 1.5 GHz, (b) Changes of resistance with repeated bending to a radius of 3 mm. Inset in (a) is SEM image and inset in (b) is an image of bending test setup. *Source:* Reprinted with permission from Reference [105]. Copyright 2016 Elsevier.

for future technology. This section provides a description of three different structured polymer composites as EMI shielding materials.

9.4.1 Foamed Structures

Foamed composites can offer substantial advantages in EMI shielding applications. First, the weight of the composite materials can be effectively decreased, which is essential in transportation applications and the fast-growing next generation of portable electronics devices. Secondly, the presence of air inside the materials decreases the real part of the permittivity, consequently reducing the reflectivity on the material surface.

Table 9.4 Properties of metal-filled polymer composites as EMI shielding materials.

Matrix/filler	Preparation method	Filler content	t (mm)	σ (S m^{-1})	SE (dB)	f (GHz)	Reference
PP/Ni	Solution mixing	10 vol.%	3	100	20	0.3	[111]
Phenolic resin/ Ni–CB	Solution mixing	50 wt%	1	31.6	85–90	1.0–15	[112]
PS/Ni–CF	Melt blending	40 phr	—	619	40	0.03–1	[113]
PVDF/Ni	Melt blending	40 vol.%	1.95	6.19×10^{-4}	20–23	8.2–12.4	[102]
PI/Cu/Ag	Solution mixing,	coating	0.01	—	55	0–1500	[105]
Epoxy/Ag–CF	Curing	4.5 wt%	2.5	—	35–38	8.2–12.4	[106]
PMMA/Ag–rGO	Solution mixing	3 vol.%	2.5	—	26.8	8.2–12.4	[107]
Epoxy/Ag	Curing	75 phr	0.04	4761	12–35	3–17	[104]
PVC/G Cu	Mechanical mixing	20 wt%	2	80	50–70	1–20	[108]
PS/Cu	Solution & melt mixing	1.79 vol.%	0.21	10^3	35~40	8.2–12.4	[109]
Glass/SnCu	Sputtering	20–40 wt%	7.1×10^{-4}	—	—	0.05–3	[110]

The first report of such systems based on PS foams filled with carbon nanofibers and carbon nanotubes were reported by Yang et al. [59, 114]. The foamed composite was formed through mixing the polymer with a chemical foaming agent (azoisobutyronitrile) in solution. Using this approach, much larger values of EMI SE were achieved compared with copper metal sheets (33 vs 10 dB cm^3 g^{-1} at frequencies 8–12 GHz). A value of 20 dB for EMI SE was achieved at much smaller filler contents with carbon nanotubes compared with carbon fibers because of their higher aspect ratios (7 vs 20 wt%, at 8–12 GHz). However, the reflectivity of carbon nanotube (CNT) foams ($T + A + R = 1\% + 18\% + 81\%$) reduced only slightly compared with unfoamed samples ($T + A + R = 0.25\% + 10.21\% + 89.54\%$) and remained as the main shielding mechanism, probably due to larger CNT content (7 wt%). In other study, polycaprolactone (PCL)/CNTs nanocomposites [115] were foamed with supercritical CO_2. A very high SE value was obtained at very low CNT content (60 dB at 0.249 vol.% and 20 dB at 0.107 vol.%, t = 2 cm). This superior performance is the result of excellent CNT dispersion and improvement of electrical conductivity upon foaming as exemplified by a foam containing 0.107 vol.% multi-walled carbon nanotubes (MWNTs) that revealed the same conductivity as an unfoamed sample with 0.16 vol.% MWNTs (Figure 9.23a). Similarly, a foamed sample including 0.249 vol.% of MWNTs exhibited conductivity twice that of an unfoamed sample filled with 0.48 vol.% of MWNTs. Moreover, the introduction of air upon foaming leads to a lower dielectric constant for a given electrical conductivity. Indeed, the dielectric constant of foamed PCL filled with 0.24 vol.% MWNT (ε_r = 3.5 at 30 GHz, Figure 9.23c) is similar to those of unfoamed PCL containing 0.16 and 0.48 vol.% MWNTs ($3 < \varepsilon_r < 4$, Figure 9.24c), although the conductivity is roughly three to four times larger (Figure 9.23a). Consequently, the foamed samples exhibited a better SE/reflectivity ratio (Figure 9.23b and d).

In another study, Eswaraiah et al. [116] reported results on foamed nanocomposites of functionalized graphene (f-G) and PVDF (Figure 9.24) with EMI SE values of 20 and 28 dB for composites containing 5 and 7 wt% f-G, respectively, in a broadband frequency range (1–8 GHz). A larger EMI SE value (28 dB) was observed for the foamed composites containing 7 wt% f-G than that for unfoamed composite (20 dB) in the X-band. This observation may be due to the skin

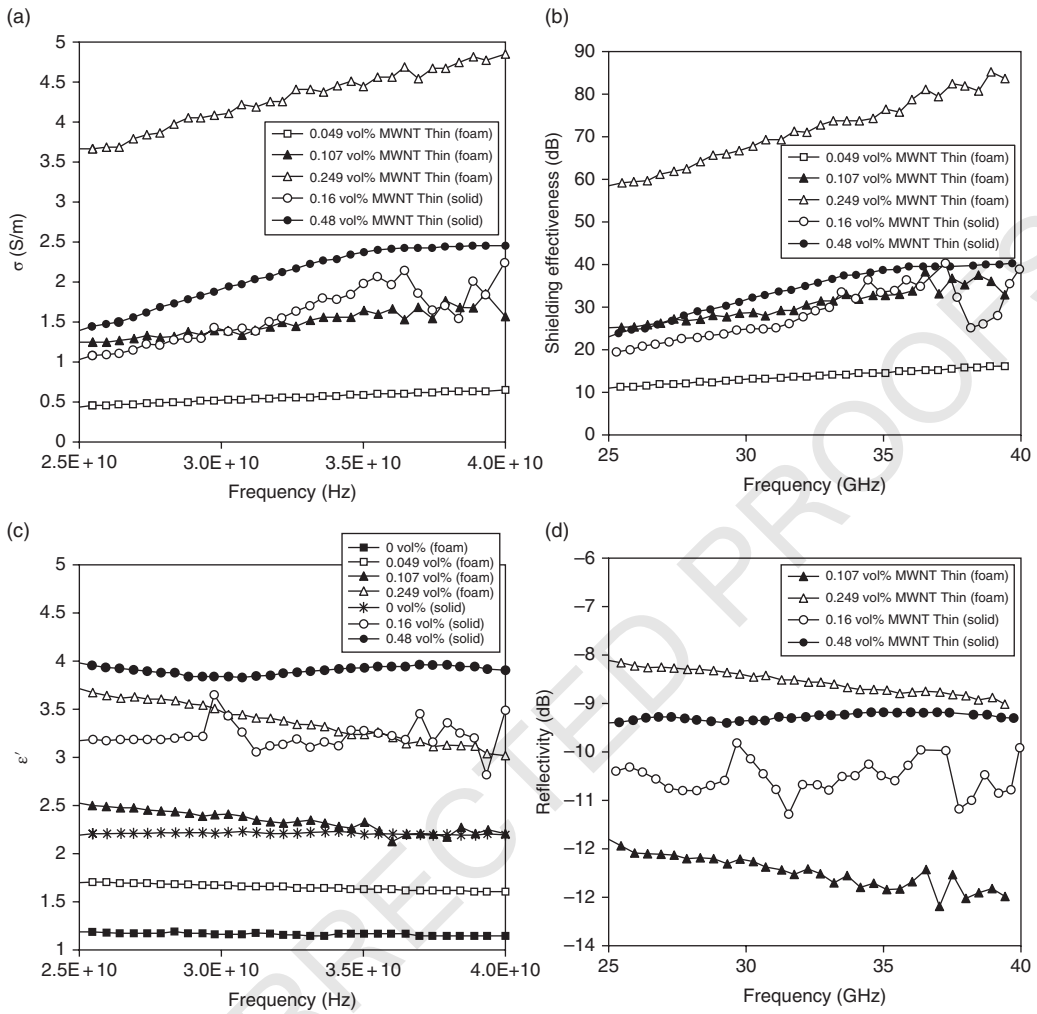

Figure 9.23 Electromagnetic properties of foamed and unfoamed MWNT/PCL nanocomposites: (a) conductivity σ, (b) shielding efficiency SE, (c) dielectric constant (ε_r), and (d) reflectivity (R).
Source: Reprinted with permission from Reference [115]. Copyright 2008 Royal Society of Chemistry.

effect of the foamed composite at higher frequencies. The increase in EMI SE value can be attributed to the increase in conductivity of the foamed composite, as graphene nanofillers establish a conducting network in the PVDF matrix. When the loading of f-G increases, the number of conducting f-G interconnections increases, resulting in more interaction and direct contacts between the nanofiller particles and incoming radiation.

Other foamed polymer composite materials were investigated using various conducting nanofillers, such as carbon black/ethylene propylene diene (EPDM) [117]; graphene sheets with PU [118], PS [60], PDMS [119], and PMMA [64]; and silver nanowires/polyimide (PI) for EMI shielding. Incorporation of high aspect ratio graphene sheets can provide a SE value of 15 dB to PMMA foams at very low content (1.8 vol.%, 8–12 GHz, t = 2.4 mm) with absorption as the main shielding mechanism [64]. Yan et al. used the salt leaching process to prepare PS foams with a high content of graphene (30 wt%) to achieve SE value of 29 dB (8–12 GHz, t = 2.5 mm) [60], which corresponds to a specific SE value of 64.4 dB cm^{-3}. Recently, Tang et al.

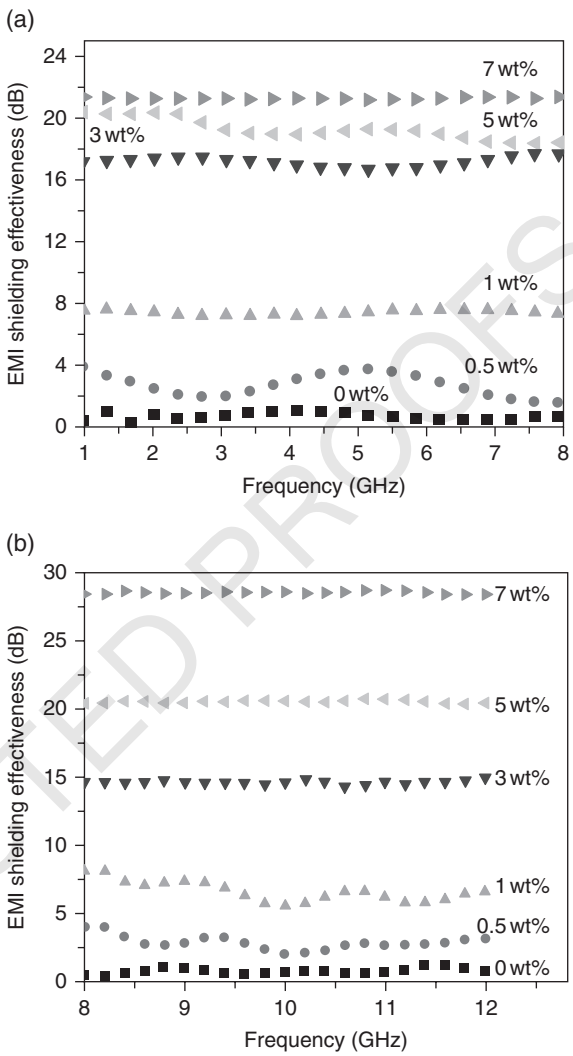

Figure 9.24 Variations of EMI SE for f-G/PVDF composites in: (a) broadband range of 1–8 GHz, (b) X-band range of 8–12 GHz. *Source:* Reprinted with permission from Reference [116]. Copyright 2011 John Wiley & Sons.

used a nickel template to deposit graphene sheets using the chemical vapor deposition method. After coating the graphene layer with PDMS and etching away the template, highly flexible foams with a low density (0.06 g cm^{-3}) were obtained, which provided high volume specific EMI SE values (500 dB cm^{-3}, 8–12 GHz, t = 1 mm) [119]. To further improve the EMI SE performance, ternary foamed composite materials were developed. Shen et al. [9] reported high-performance PEI/graphene@Fe_3O_4 composite foams with flexible character and low density of about 0.28–0.4 g cm^{-3} using a phase separation method. The obtained PEI/G@Fe_3O_4 foam with a G@Fe_3O_4 loading of 10 wt% exhibited an excellent specific EMI SE value of 41.5 dB cm^3·g^{-1} at 8–12 GHz.

Furthermore, ultra-lightweight polyimide (PI) composites filled with three different shapes of silver nanofillers, nanospheres (AgNSs), nanowires (AgNWs), and nanowires–nanoplatelets (AgNWPs), were fabricated through a facile and effective one-pot liquid foaming process [120]. It was observed that, at the same filler content, the EMI SE values of the foamed composites decreased in the following order: AgNWPs > AgNWs > AgNSs (Figure 9.25). The sample names were designated as (PIF-WS) for AgNWPs, (PIF-W) for AgNWs, and (PIF-P)

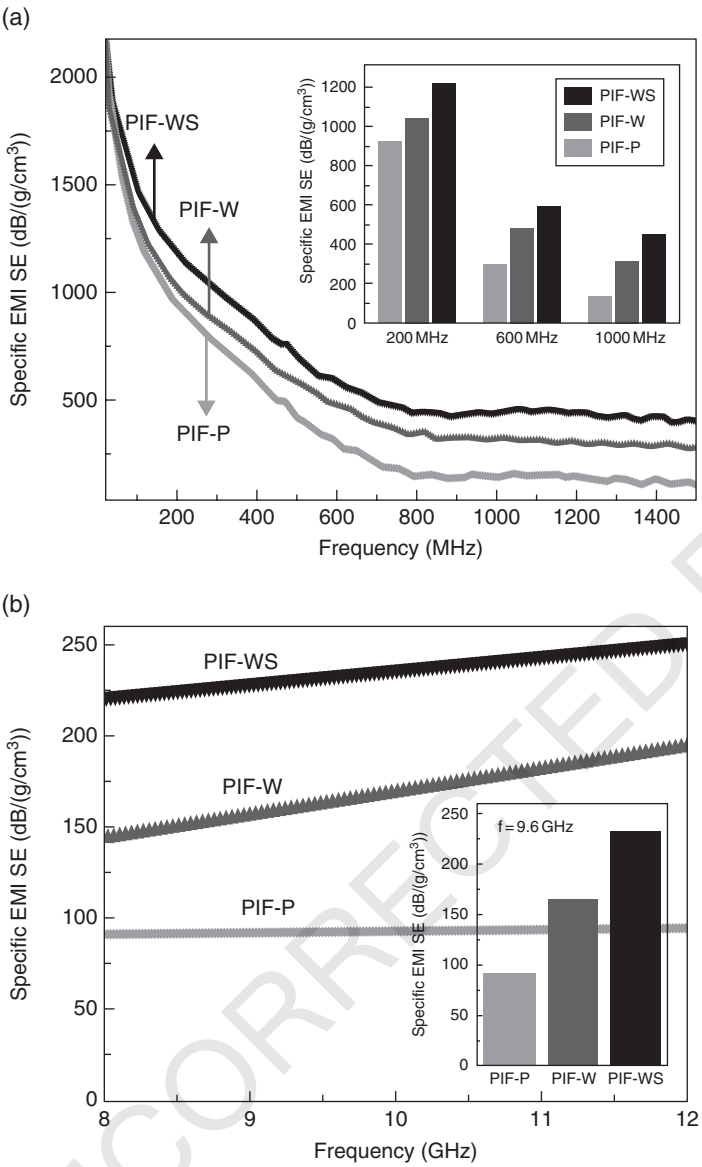

Figure 9.25 Specific EMI SE of foamed composites of PI-P, PI-W, and PI-WS measured in frequency ranges of (a) 30 MHz to 1.5 GHz and (b) 8–12 GHz. Inset (a) specific EMI SE values at 200, 600, and 1000 MHz. Inset (b) specific EMI SE values of foamed composites at 9.6 GHz. *Source:* Reprinted with permission from Reference [120]. Copyright 2015 Royal Society of Chemistry.

for AgNSs. Foamed AgNWPs composite exhibited the largest EMI SE value owing to the denser 3D conductive network of AgNWPs compared with AgNWs and AgNSs. This performance is attributed to the fact that AgNWPs interconnect with each other to form a dense and interconnected network in polymer matrix due to its large aspect ratio and AgNWs bridging effects for silver nanoplatelets, which provides a fast electron transport pathway. Maximum specific EMI SE values of 1208 dB cm^3 g^{-1} at 200 MHz, 650 dB cm^3 g^{-1} at 600 MHz, 488 dB cm^3 g^{-1} in the frequency range of 800–1500 MHz, and 216–249 dB cm^3 g^{-1} at 8–12 GHz

Table 9.5 Specific EMI SE values of various foamed materials measured in the X-band frequency range. [121]. Reproduced with permission of the American Chemical Society.

Material	Filler content	*t* (mm)	SE (dB)	Specific EMI SE ($dB \cdot cm^3 g^{-1})^{-1}$	Specific EMI SE divided by thickness ($dB \cdot cm^3 g^{-1} mm^{-1}$)
PDMS/rGO	0.8 wt%	1.0	20	333	333
PS/rGO	30 wt%	2.5	29	64.4	25.7
PP/SSF	1.1 vol.%	3.1	48	75	24.2
PEI/rGO	10 wt%	2.3	13	44	19.2
PEI/rGO/Fe_3O_4	10 wt%	2.5	17	42	16.8
Fluorocarbon/CNT	12 wt%	3.8	42–48	50–57	13.2–15.0
PP/CF	10 vol.%	3.1	25	34	10.9
PCL/MWCNT	2 wt%	20	60–80	193–258	9.7–12.9
PMMA/rGO	1.8 vol.%	2.4	19	24	10.0
PS/CNT	7 wt%	N/A	19	33	N/A
PS/CNF	15 wt%	N/A	19	N/A	N/A
PVDF/graphene	2 wt%	N/A	28	N/A	N/A

were achieved in the foamed composite containing 4.5 wt% AgNWPs, which far surpasses the best values of other composite materials.

Lightweight PP composite foam with stainless-steel fiber (PP–SSF) was fabricated using a foam injection molding process [121]. A maximum specific EMI SE value of 75 dB $cm^3 g^{-1}$ was achieved in a sample containing 1.1 vol.% SSF, which is much larger than that of the solid counterpart. Foamed and solid PP/CF composites containing various CF contents (0–10 vol.%) were prepared using dissolved pressurized nitrogen gas [39]. At 10 vol.% CF, the SE value for the foamed composites reached about 24.9 dB, corresponding to 99.7% blocking of electromagnetic waves in the X-band frequency range. At the same CF content, the solid composites presented a SE value of about 19.8 dB. At even 7.5 vol.% CF content, the SE value of foamed composites reached 16.3 dB, which is in the range required for computer devices (15–20 dB) [122]. Compared with the similar level of EM blocking reported for 7 wt% MWCNT [123], using 7.5–10 vol.% CF in the foamed composites suggests an economical alternative. The EMI SE values for the foamed materials reported in the literature are summarized in Table 9.5.

9.4.2 Sandwiched Structures

Sandwiched composite structures have been applied with a polymer matrix to realize a class of lightweight structures capable of shielding EMI. However, very few studies report use of the concept of sandwiched materials for designing such EMI shielding materials capable of being used as a weight efficient load-bearing structures. Sandwich design, with a lightweight core in between high-stiffness skins face-sheets, not only offers superior strength, modulus, and rigidity to weight ratio but also provides scope for intelligently incorporating multifunctionalities in the structure by careful selection of various material design parameters, like chemistry of the matrix, nature and thickness of the core and skins, and core to sandwich thickness ratio. Multilayer graphene sheets (MLG) along with paraffin wax and PVA were used in the fabrication of sandwich structures [54]. As expected, the sandwich structures with higher MLG loadings showed enhanced SE (Figure 9.26a). The greatest EMI SE value was 14 dB for sandwich structures with 60 vol.% MLG.

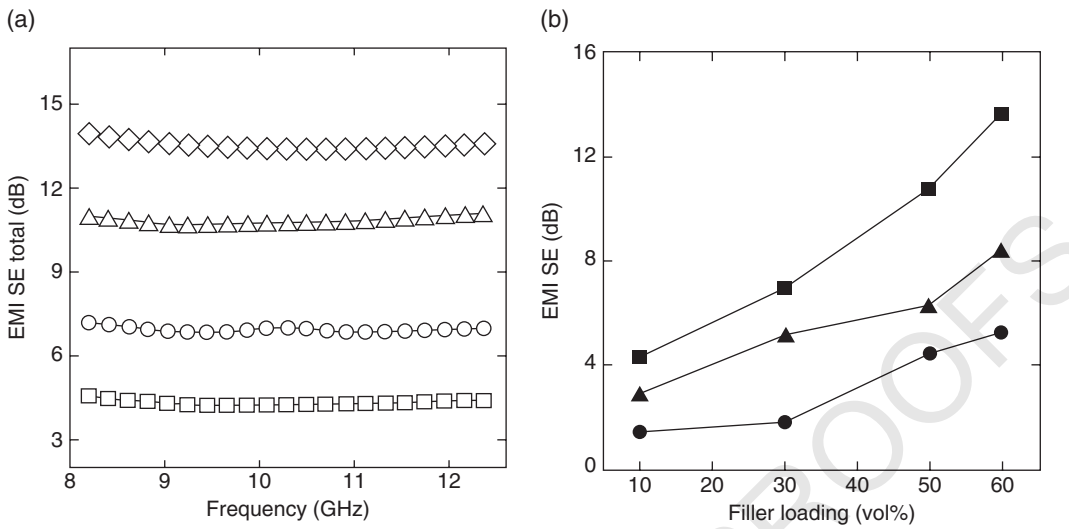

Figure 9.26 (a) Total EMI SE values of as-fabricated sandwich structures with G–E films of different MLG loadings: 10 (-□-), 30 (-○-), 50 (-△-), and 60 (-◇-) vol.%. (b) Absorption shielding (-●-), reflection shielding (-▲-), and total EMI SE (-■-) coefficients of the sandwich structures coated with G–E films with different MLG loadings at 9 GHz. *Source:* Adapted with permission from Reference [54]. Copyright 2014 Elsevier.

Figure 9.26b exhibits variations of the corresponding coefficients at 9 GHz, suggesting higher reflection shielding in the as-fabricated sandwich structures in the investigated range.

Flexible transparent poly(ether sulfone) (PES)/silver nanowires/PET sandwich-structured films have also been reported for high efficiency EMI shielding material [124]. EMI SE values up to 38 dB could be achieved, which is much larger than 20 dB required in commercial applications and also much better than the performance of many conductive polymer composites and carbon-based conductive films. Silver nanowires can readily meet these requirements. Moreover, silver nanowires can be homogeneously paved on flexible substrates to construct conductive networks with good light transmission so as to obtain free-standing flexible transparent conductive films for applications where good transparency is required, such as the protective covers of keyboards, displays, and observation windows, to shield EMI from the outside and EM radiation from themselves. Dasgupta et al. [125] developed epoxy-based sandwich composites for high performance EMI shielding. The SE values of the sandwich materials over the frequency band (Figure 9.27) indicate that the presence of metallic (aluminum/copper) mesh layers in the face-sheets significantly improves the shielding capabilities well above 60 dB, almost up to 90 dB in certain frequencies. The results conclusively demonstrated the efficiency of all the sandwich materials for applications demanding moderate (40 dB) to very large (>60 dB) EMI SE.

9.4.3 Segregated Structures

The formation of segregated structures can improve electrical conductivity and EMI SE; however, few reports concerning shielding materials based on segregated conducting polymer composites (s-CPCs) have been published. In such architectures, electrical nanofillers are distributed only at the interfaces of polymer granules rather than homogeneously distributed in the whole volume of the polymer matrix. Graphene was first used to construct segregated conductive networks in a UHMWPE matrix, exhibiting an electrical conductivity of 0.04 S m^{-1} at a rather small content of

ID	Matrix	Skin	Core	*t*	*d**
				mm	g/cc
SW-01	Matrix A	Carbon	Insulating syntactic foam	2.75	0.76
SW-02	Matrix A	Al. mesh-glass	Insulating syntactic foam	2.75	0.81
HSW-01	Matrix B	Al. mesh-glass	Insulating syntactic foam	2.60	0.71
HSW-02	Matrix B	Cu. mesh-carbon	Insulating syntactic foam	2.62	0.70
HSW-03	Matrix B	Cu. mesh-carbon	Conducting syntactic foam	2.20	0.81

t = thickness *d* = density

* Effective density calculated from the mass of sandwich sample

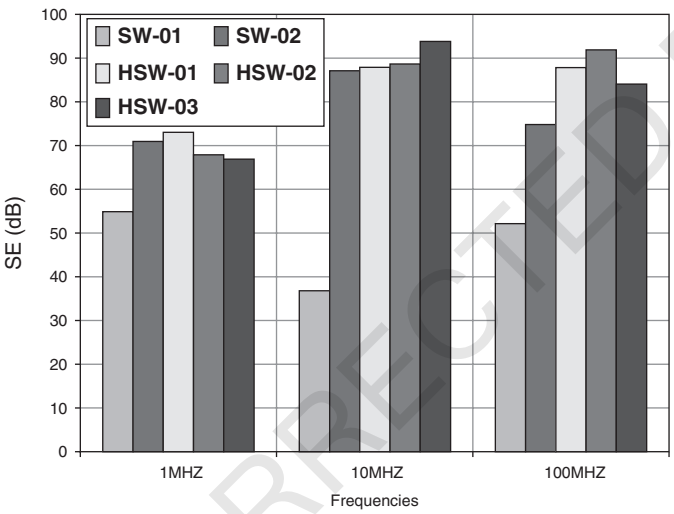

Figure 9.27 Details of sandwich composites and their EMI shielding capabilities. Matrix A: novolac based epoxy; matrix B: diglycidyl ether of bisphenol-A (DGEBA) based epoxy. *Source:* Reprinted with permission from Reference [125]. Copyright 2008 IEEE.

0.6 vol.% [126]. Variation of EMI SE over the frequency range 8.2–12.4 GHz for thermally reduced graphene oxide (TRGO) segregated composites with UHMWPE is shown in Figure 9.28a [62]. All examined composites exhibited weak frequency dependent EMI SE performance; EMI SE increased greatly with TRGO content. The composite containing only 0.660 vol.% (or 1.50 wt%) TRGO showed an EMI SE of 28.3–32.4 dB over the frequency range, the greatest EMI SE value reported so far for graphene/polymer composites at such a low level of graphene content.

Although the formation of such segregated architectures could improve electrical and EMI SE performance, one major issue is that the existence of nanofiller agglomerates at polymer granule interfaces restricts molecular diffusion between granules, leading to weak mechanical performance of the segregated materials and restricting their applications. Recently, Yan et al. reported a high-performance EMI SE composite based on reduced graphene oxide (rGO) and PS fabricated via high pressure solid-phase compression molding [61]. The superior EMI SE

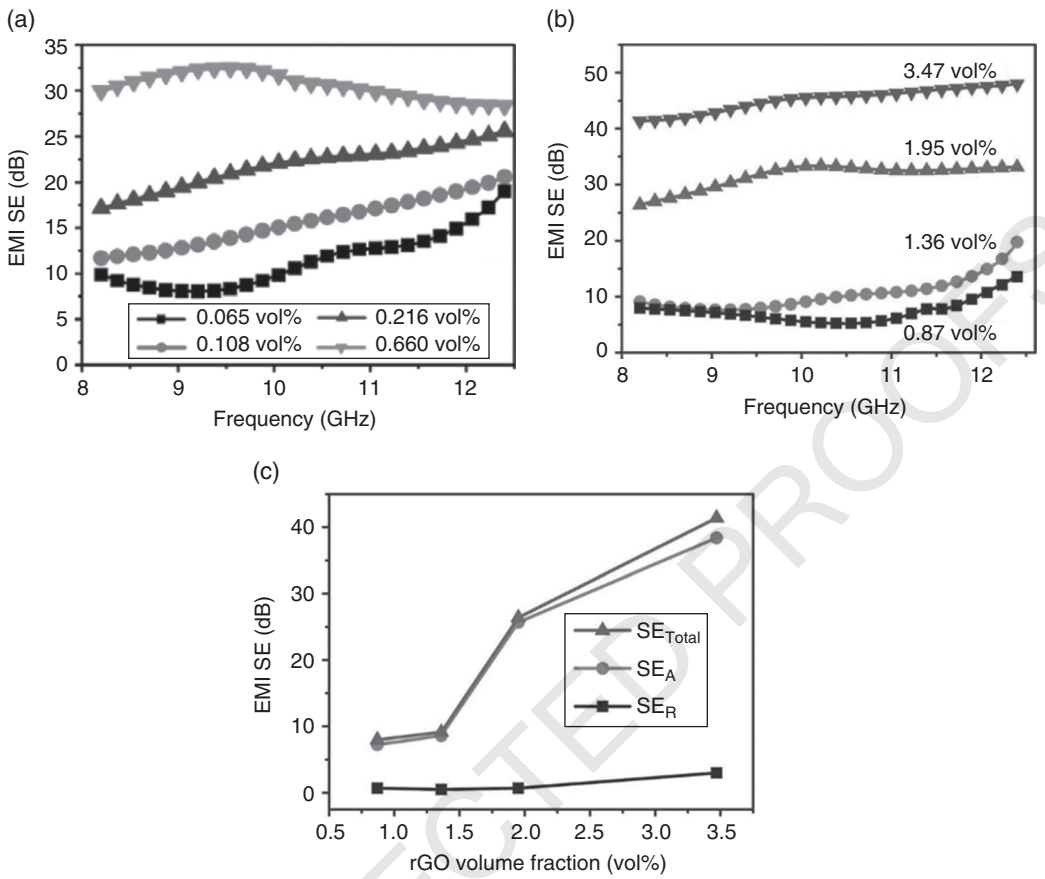

Figure 9.28 Variations of EMI SE as a function of frequency in the X band for: (a) TRGO/UHMWPE segregated composites with various TRGO contents [62], (b) rGO/PS composites with various rGO contents, and (c) variations of EMI SE as a function of volume fraction for rGO/PS composites. *Source:* Adapted with permission from Reference [61 and 62]. Copyright 2015 John Wiley & Sons and 2014 IOP Science.

value of 45.1 dB, the largest value among rGO-based polymer composites, was achieved with only 3.47 vol.% rGO loading owning to a multi-facet segregated architecture with rGO selectively located on the boundaries among PS multi-facets (Figure 9.28b). This special architecture not only provides many interfaces to absorb the EM waves (Figure 9.28c), but also dramatically reduces the loading of rGO through confining rGO at the interfaces. In another study, a satisfactory EMI SE value as high as 38 dB with only 1.8 vol.% copper nanowires (CuNWs) in CuNW/PS s-CPCs was obtained [109, 122]. Pang et al. fabricated GNS/PS s-CPCs through solid-phase high pressure molding to achieve EMI SE values up to 45.1 dB at a relatively low graphene nanosheets (GNSs) loading of 3.47 vol.% [127].

9.5 Future Perspectives

As we have reviewed here, two main approaches have been attempted to enhance the EMI SE properties of polymer composites. One is to develop new materials with high electrical conductivity and electromagnetic attribution and the other one is to develop new structures based

on the "structure or design" strategy of materials to achieve required EMI SE properties. Over the last two decades, materials scientists have proposed new and versatile materials to suit the EMI shielding requirements. Starting from the use of metal mesh and films to the recent advent of carbon-based materials, researchers have devoted significant efforts on this subject to challenge the ever growing concern of EMI shielding. However, there is still a long way to go as the use of communication devices will keep on growing in the coming years and the need to mitigate the EMI problems will require due attention.

While designing a commercial product, the absolute EMI SE values will retain its significance whereas the cost factor cannot be ignored. There is yet no absolute commercial substitute for metals, such as silver, copper, aluminum, and iron, as these carry the largest share of the EMI shielding market due to their superior shielding properties. Other materials can take market share only if they provide better properties or offer significant cost advantage. The most investigated materials in recent decades, for instance, ferrites, carbon materials, magnetic oxides, and conducting polymers, are all good and carry the possibility of commercial use; nevertheless, there is still plenty of opportunity to look beyond the stage where we have reached. To advance the idea into realization, researchers will need to think of discovering new materials that could tackle the ballistic surge of EMI about to happen in coming years. Graphene, as the most investigated material in the past ten years, is yet to deliver the full characteristics it possesses. Recent research and review articles present the possibility of using pristine graphene as EMI shielding material; nevertheless, the way to explore the full potential of this wonderful material still awaits big ideas. Graphene can be an ideal substitute if properties of products like scotch-tape can be reached at mass production scale at low cost. Scientists will need to explore how to achieve these goals. Once this challenge is met, the dream to protect human beings from the adverse effects of EM radiations and to keep the smooth working of equipment will be realized in the near future. Despite the significant advances in research, we have not come across a material having both the high electrical conductivity and high magnetic attributes.

The other option to enhance EMI shielding is through altering the structural design of the shielding products. We have already witnessed several novel designs based on sandwiched type structures, nacre-like films, foamed structures, segregated structures, and others. Apart from materials with good EM attributes, the factor that can greatly influence the EM waves is how it is dealt with inside the structure of shielding material. There are already wonderful reports highlighting the influence of designing novel structures – nevertheless the opportunities are limitless. Nature has always inspired human beings, scientists in particular. Honeycomb type structures are the latest addition to the ever growing list of EMI shielding materials. Similar designs, taking inspiration from nature, could be further explored in future to take advantage of what already exists.

References

1 Thomassin, J.-M., Jérôme, C., Pardoen, T. et al. (2013). *Materials Science and Engineering: R: Reports* 74: 211–232.
2 Geetha, S., Satheesh Kumar, K. K., Rao, C. R. K. et al. (2009). *Journal of Applied Polymer Science* 112: 2073–2086.
3 Wang, Y. and Jing, X. (2005). *Polymers for Advanced Technologies* 16: 344–351.
4 Chung, D. D. L. (2000). *Journal of Materials Engineering and Performance* 9: 350–354.
5 Chung, D. D. L. (2001). *Carbon* 39: 279–285.
6 Moitra, D., Hazra, S., Ghosh, B. K. et al. (2015). *RSC Advances* 5: 51130–51134.

7 Zhu, W., Wang, L., Zhao, R. et al. (2011). *Nanoscale* 3: 2862–2864.
8 Chung, D. D. L. (2012). *Carbon* 50: 3342–3353.
9 Shen, B., Zhai, W., Tao, M. et al. (2013). *ACS Applied Materials & Interfaces* 5: 11383–11391.
10 Xu, P., Han, X., Wang, C. et al. (2008). *The Journal of Physical Chemistry B* 112: 2775–2781.
11 Hosseini, S. H., Mohseni, S. H., Asadnia, A., and Kerdari, H. (2011). *Journal of Alloys and Compounds* 509: 4682–4687.
12 Li, Y., Yi, R., Yan, A. et al. (2009). *Solid State Sciences* 11: 1319–1324.
13 Pawar, S. P., Stephen, S., Bose, S., and Mittal, V. (2015). *Physical Chemistry Chemical Physics* 17: 14922–14930.
14 Dhakate, S. R., Subhedar, K. M., and Singh, B. P. (2015). *RSC Advances* 5: 43036–43057.
15 Shen, B., Zhai, W., and Zheng, W. (2014). *Advanced Functional Materials* 24: 4542–4548.
16 Cao, M.-S., Wang, X.-X., Cao, W.-Q., and Yuan, J. (2015). *Journal of Materials Chemistry C* 3: 6589–6599.
17 Song, W.-L., Fan, L.-Z., Cao, M.-S. et al. (2014). *Journal of Materials Chemistry C* 2: 5057–5064.
18 Jiang, X., Yan, D.-X., Bao, Y. et al. (2015). *RSC Advances* 5: 22587–22592.
19 Jia, L.-C., Yan, D.-X., Cui, C.-H. et al. (2015). *Journal of Materials Chemistry C* 3: 9369–9378.
20 Huo, J., Wang, L., and Yu, H. (2009). *Journal of Materials Science* 44: 3917–3927.
21 Yousefi, N., Sun, X., Lin, X. et al. (2014). *Advanced Materials* 26: 5480–5487.
22 Bingqing, Y., Liming, Y., Leimei, S. et al. (2012). *Journal of Physics D: Applied Physics* 45: 235108.
23 Shahzad, F., Yu, S., Kumar, P. et al. (2015). *Composite Structures* 133: 1267–1275.
24 Krueger, Q. J. and King, J. A. (2003). *Advances in Polymer Technology* 22: 96–111.
25 Zhang, Y., Wang, Z., Zhang, B. et al. (2015). *RSC Advances* 5: 93499–93506.
26 (a) Hong, Y. K., Lee, C. Y., Jeong, C. K. et al. (2003). *Review of Scientific Instruments* 74: 1098–1102. (b) Kumar, K. K., Geetha, S., and Trivedi, D. C. *Current Applied Physics* 2005 (5): 603–608.
27 Katsumi, Y., Munehiro, T., Keiichi, K., and Toshiyuki, O. (1985). *Japanese Journal of Applied Physics* 24: L693.
28 Wu, F., Xu, Z., Wang, Y., and Wang, M. (2014). *RSC Advances* 4: 38797–38803.
29 Chiang, C. K., Fincher, C. R., Park, Y. W. et al. (1977). *Physical Review Letters* 39: 1098–1101.
30 Trivedi, D. C. and Dhawan, S. K. (1993). *Synthetic Metals* 59: 267–272.
31 Machida, S., Miyata, S., and Techagumpuch, A. (1989). *Synthetic Metals* 31: 311–318.
32 (a) Yoshino, K., Tabata, M., Kaneto, K., and Ohsawa, T. (1985). *Japanese Journal of Applied Physics* 24: L693. (b) Kaynak, A., Unsworth, J., Clout, R. et al. (1994). *Journal of Applied Polymer Science* 3: 269–278.
33 Panwar, V. and Mehra, R. M. (2008). *Polymer Engineering & Science* 48: 2178–2187.
34 Hu, H., Zhang, G., Xiao, L. et al. (2012). *Carbon* 50: 4596–4599.
35 Sachdev, V. K., Patel, K., Bhattacharya, S., and Tandon, R. P. (2011). *Journal of Applied Polymer Science* 120: 1100–1105.
36 Nanni, F., Travaglia, P., and Valentini, M. (2009). *Composites Science and Technology* 69: 485–490.
37 Al-Saleh, M. H. and Sundararaj, U. (2013). *Polymer International* 62: 601–607.
38 Markham, D. (1999). *Materials & Design* 21: 45–50.
39 Ameli, A., Jung, P. U., and Park, C. B. (2013). *Carbon* 60: 379–391.
40 Singh, B. P., Prasanta, V. C., Saini, P. et al. (2013). *Journal of Nanoparticle Research* 15: 1–12.
41 Gupta, A. and Choudhary, V. (2011). *Composites Science and Technology* 71: 1563–1568.
42 Das, N., Chaki, T., Khastgir, D., and Chakraborty, A. (2001). *Advances in Polymer Technology* 20: 226–236.

43 Rahaman, M., Chaki, T., and Khastgir, D. (2011). *Journal of Materials Science* 46: 3989–3999.
44 Aal, N. A., El-Tantawy, F., Al-Hajry, A., and Bououdina, M. (2008). *Polymer Composites* 29: 125–132.
45 Mohanraj, G., Chaki, T., Chakraborty, A., and Khastgir, D. (2004). *Journal of Applied Polymer Science* 92: 2179–2188.
46 Im, J. S., Kim, J. G., and Lee, Y.-S. (2009). *Carbon* 47: 2640–2647.
47 Mohammed, H. A.-S. and Uttandaraman, S. (2013). *Journal of Physics D: Applied Physics* 46: 035304.
48 Kuester, S., Merlini, C., Barra, G. M. O. et al. (2016). *Composites Part B: Engineering* 84: 236–247.
49 Liang, J., Wang, Y., Huang, Y. et al. (2009). *Carbon* 47: 922–925.
50 Shahzad, F., Kumar, P., Yu, S. et al. (2015). *Journal of Materials Chemistry C* 3: 9802–9810.
51 Kumar, P., Shahzad, F., Yu, S. et al. (2015). *Carbon* 94: 494–500.
52 Basavaraja, C., Kim, W. J., Kim, Y. D., and Huh, D. S. (2011). *Materials Letters* 65: 3120–3123.
53 Tung, T. T., Feller, J.-F., Kim, T. et al. (2012). *Journal of Polymer Science Part A: Polymer Chemistry* 50: 927–935.
54 Song, W.-L., Cao, M.-S., Lu, M.-M. et al. (2014). *Carbon* 66: 67–76.
55 Puri, P., Mehta, R., and Rattan, S. (2015). *Journal of Electronic Materials* 44: 4255–4268.
56 De Bellis, G., Tamburrano, A., Dinescu, A. et al. (2011). *Carbon* 49: 4291–4300.
57 Maiti, S., Shrivastava, N. K., Suin, S., and Khatua, B. B. (2013). *ACS Applied Materials & Interfaces* 5: 4712–4724.
58 Arjmand, M., Apperley, T., Okoniewski, M., and Sundararaj, U. (2012). *Carbon* 50: 5126–5134.
59 Yang, Y., Gupta, M. C., Dudley, K. L., and Lawrence, R. W. (2005). *Nano Letters* 5: 2131–2134.
60 Yan, D.-X., Ren, P.-G., Pang, H. et al. (2012). *Journal of Materials Chemistry* 22: 18772–18774.
61 Yan, D.-X., Pang, H., Li, B. et al. (2015). *Advanced Functional Materials* 25: 559–566.
62 Ding-Xiang, Y., Huan, P., Ling, X. et al. (2014). *Nanotechnology* 25: 145705.
63 Zhang, H.-B., Zheng, W.-G., Yan, Q. et al. (2012). *Carbon* 50: 5117–5125.
64 Zhang, H.-B., Yan, Q., Zheng, W.-G. et al. (2011). *ACS Applied Materials & Interfaces* 3: 918–924.
65 Ling, J., Zhai, W., Feng, W. et al. (2013). *ACS Applied Materials & Interfaces* 5: 2677–2684.
66 Chen, Z., Xu, C., Ma, C. et al. (2013). *Advanced Materials* 25: 1296–1300.
67 Chen, D., Wang, G.-S., He, S. et al. (2013). *Journal of Materials Chemistry A* 1: 5996–6003.
68 Kong, L., Yin, X., Zhang, Y. et al. (2013). *The Journal of Physical Chemistry C* 117: 19701–19711.
69 Ren, Y.-L., Wu, H.-Y., Lu, M.-M. et al. (2012). *ACS Applied Materials & Interfaces* 4: 6436–6442.
70 Cao, M.-S., Yang, J., Song, W.-L. et al. (2012). *ACS Applied Materials & Interfaces* 4: 6949–6956.
71 Yuan, B., Bao, C., Qian, X. et al. (2014). *Carbon* 75: 178–189.
72 Guan, H., Liu, S., Zhao, Y., and Duan, Y. (2006). *Journal of Electronic Materials* 35: 892–896.
73 Bayat, M., Yang, H., Ko, F. K. et al. (2014). *Polymer* 55: 936–943.
74 Singh, K., Ohlan, A., Pham, V. H. et al. (2013). *Nanoscale* 5: 2411–2420.
75 Dhawan, S. K., Singh, K., Bakhshi, A. K., and Ohlan, A. (2009). *Synthetic Metals* 159: 2259–2262.
76 He, Z., Fang, Y., Wang, X., and Pang, H. (2011). *Synthetic Metals* 161: 420–425.
77 Xiao, H. and Yuan-Sheng, W. (2007). *Physica Scripta* 2007: 335–339.
78 Singh, A. P., Mishra, M., Sambyal, P. et al. (2014). *Journal of Materials Chemistry A* 2: 3581–3593.
79 Hosseini, S. H. and Asadnia, A. (2012). *Journal of Nanomaterials* 2012: 198973.

80 Xiao, H.-M., Zhang, W.-D., and Fu, S.-Y. (2010). *Composites Science and Technology* 70: 909–915.
81 Singh, K., Ohlan, A., Saini, P., and Dhawan, S. K. (2008). *Polymers for Advanced Technologies* 19: 229–236.
82 Li, B.-W., Shen, Y., Yue, Z.-X., and Nan, C.-W. (2006). *Applied Physics Letters* 89: 132504.
83 Zhu, J., Wei, S., Haldolaarachchige, N. et al. (2011). *The Journal of Physical Chemistry C* 115: 15304–15310.
84 Xu, P., Han, X., Wang, C. et al. (2008). *The Journal of Physical Chemistry B* 112: 10443–10448.
85 Unsworth, J., Kaynak, A., Lunn, B. A., and Beard, G. E. (1993). *Journal Materials Science* 28: 3307–3312.
86 Chen, D., Quan, H., Huang, Z. et al. (2014). *Composites Science and Technology* 102: 126–131.
87 Zhang, X.-J., Wang, G.-S., Cao, W.-Q. et al. (2014). *ACS Applied Materials & Interfaces* 6: 7471–7478.
88 Wang, G.-S., Wu, Y., Wei, Y.-Z. et al. (2014). *ChemPlusChem* 79: 375–381.
89 Varshney, S., Ohlan, A., Jain, V. K. et al. (2014). *Industrial & Engineering Chemistry Research* 53: 14282–14290.
90 Chen, Y., Wang, Y., Zhang, H.-B. et al. (2015). *Carbon* 82: 67–76.
91 Crespo, M., Méndez, N., González, M. et al. (2014). *Carbon* 74: 63–72.
92 Zhang, T., Huang, D., Yang, Y. et al. (2013). *Materials Science and Engineering: B* 178: 1–9.
93 Yao, K., Gong, J., Tian, N. et al. (2015). *RSC Advances* 5: 31910–31919.
94 Bai, X., Zhai, Y., and Zhang, Y. (2011). *The Journal of Physical Chemistry C* 115: 11673–11677.
95 Gupta, A., Singh, A. P., Varshney, S. et al. (2014). *RSC Advances* 4: 62413–62422.
96 Wang, Y., Wu, X., Zhang, W., and Huang, S. (2015). *Synthetic Metals* 210: 165–170.
97 Sui, M., Lü, X., Xie, A. et al. (2015). *Synthetic Metals* 210: 156–164.
98 Ohlan, A., Singh, K., Chandra, A., and Dhawan, S. K. (2010). *ACS Applied Materials & Interfaces* 2: 927–933.
99 Eda, G., Fanchini, G., and Chhowalla, M. (2008). *Nature Nanotechnology* 3: 270–274.
100 Zhu, Y., Stoller, M. D., Cai, W. et al. (2010). *ACS Nano* 4: 1227–1233.
101 Murugan, A. V., Muraliganth, T., and Manthiram, A. (2009). *Chemistry of Materials* 21: 5004–5006.
102 Gargama, H., Thakur, A. K., and Chaturvedi, S. K. (2015). *Journal of Applied Physics* 117: 224903.
103 Panda, M., Srinivas, V., and Thakur, A. K. (2008). *Applied Physics Letters* 92: 132905.
104 Yu, Y.-H., Ma, C.-C. M., Teng, C.-C. et al. (2012). *Materials Chemistry and Physics* 136: 334–340.
105 Kim, D.-H., Kim, Y., and Kim, J.-W. (2016). *Materials & Design* 89: 703–707.
106 Li, J., Qi, S., Zhang, M., and Wang, Z. (2015). *Journal of Applied Polymer Science* 132: 42306.
107 Long, T., Hu, L., Dai, H., and Tang, Y. (2014). *Applied Physics A* 116: 25–32.
108 Al-Ghamdi, A. A. and El-Tantawy, F. (2010). *Composites Part A: Applied Science and Manufacturing* 41: 1693–1701.
109 Gelves, G. A., Al-Saleh, M. H., and Sundararaj, U. (2011). *Journal of Materials Chemistry* 21: 829–836.
110 Hung, F.-S., Hung, F.-Y., and Chiang, C.-M. (2011). *Applied Surface Science* 257: 3733–3738.
111 Wenderoth, K., Petermann, J., Kruse, K. D. et al. (1989). *Polymer Composites* 10: 52–56.
112 El-Tantawy, F., Aal, N. A., and Sung, Y. K. (2005). *Macromolecular Research* 13: 194–205.
113 Chiang, W.-Y. and Ao, J.-Y. (1995). *Journal of Polymer Research* 2: 83–89.
114 Yang, Y., Gupta, M. C., Dudley, K. L., and Lawrence, R. W. (2005). *Advanced Materials* 17: 1999–2003.
115 Thomassin, J.-M., Pagnoulle, C., Bednarz, L. et al. (2008). *Journal of Materials Chemistry* 18: 792–796.

116 Eswaraiah, V., Sankaranarayanan, V., and Ramaprabhu, S. (2011). *Macromolecular Materials and Engineering* 296: 894–898.
117 Mahapatra, S. P., Sridhar, V., and Tripathy, D. K. (2008). *Polymer Composites* 29: 465–472.
118 Bernal, M. M., Molenberg, I., Estravis, S. et al. (2012). *Journal of Materials Science* 47: 5673–5679.
119 Tang, Q., Zhou, Z., and Chen, Z. (2013). Nanoscale (5): 4541–4583.
120 Ma, J., Wang, K., and Zhan, M. (2015). *RSC Advances* 5: 65283–65296.
121 Ameli, A., Nofar, M., Wang, S., and Park, C. B. (2014). *ACS Applied Materials & Interfaces* 6: 11091–11100.
122 Al-Saleh, M. H., Gelves, G. A., and Sundararaj, U. (2011). *Composites Part A: Applied Science and Manufacturing* 42: 92–97.
123 Yang, Y., Gupta, M. C., Dudley, K. L., and Lawrence, R. W. (2005). *Journal of Nanoscience and Nanotechnology* 5: 927–931.
124 Hu, M., Gao, J., Dong, Y. et al. (2012). *Langmuir* 28: 7101–7106.
125 S. Dasgupta, K. R. Sekhar, B. N. Ravishankar, M. Kumar and S. Sankaran, Abstracts of the 10th international conference on electromagnetic interference and compatibility (INCEMIC 2008), Bangalore, 26-27 Nov. 2008.
126 Pang, H., Chen, T., Zhang, G. et al. (2010). *Materials Letters* 64: 2226–2229.
127 Pang, H., Xu, L., Yan, D.-X., and Li, Z.-M. (2014). *Progress in Polymer Science* 39: 1908–1933.